Organic & Biomolecular Chemistry

ROYAL SOCIETY OF CHEMISTRY

REVIEW

View Article Online
View Journal | View Issue

Cite this: *Org. Biomol. Chem.*, 2021, **19**, 5254

Antitumor activity of tridentate pincer and related metal complexes

Shulei Wu,† Zaoduan Wu,† Qianyi Ge, Xing Zheng* and Zehua Yang *

Received 25th March 2021,
Accepted 4th May 2021

DOI: 10.1039/d1ob00577d

rsc.li/obc

Pincer complexes featuring tunable tridentate ligand frameworks are one of the most actively studied classes of metal-based complexes. Currently, growing attention is devoted to the cytotoxicity of pincer and related metal complexes. The antiproliferative activity of numerous pincer complexes has been reported. Pincer tridentate ligand scaffolds show different coordination modes and offer multiple options for directed structural modifications. This review summarizes the significant progress in the research studies of the antitumor activity of pincer and related platinum(II), gold(III), palladium(II), copper(II), iron(III), ruthenium(II), nickel(II) and some other metal complexes, in order to provide a reference for designing novel metal coordination drug candidates with promising antitumor activity.

1 Introduction

Cancer is one of the most serious diseases that threaten human health. Approximately 18.1 million new cancer cases and 9.6 million cancer deaths were reported worldwide in 2018.[1] Chemotherapy is the main method of cancer treatment. Since cisplatin was approved by the FDA in the 1970s,[2] it has been widely used in treating a variety of solid tumors as the first metal coordination compound. However, its side effects and drug resistance are great challenges for clinical application.[3] Although the second-generation drug carboplatin and the third-generation drug oxaliplatin have improved stability and are less toxic to normal cells than cisplatin, their cytotoxicity is not as good as that of cisplatin.[4] Therefore, the development of new metal coordination compounds with better antitumor activity and lower side effects is a common concern of researchers.

Pincer metal complexes (Fig. 1) formed by the coordination of tridentate ligands and transition metals have attracted extensive attention. This special structure not only improves the stability of metal coordination compounds against biological reduction and ligand exchange reactions, but also combines the characteristics of metallic centers and organic scaffolds.[5] The easy regulation of the electrical properties of pincer ligands provides convenience for various modifications in metal coordinated compounds. The multiple coordination sites of transition metals also make possible the introduction

Hunan Provincial Key Laboratory of Tumor Microenvironment Responsive Drug Research, Hunan Province Cooperative Innovation Center for Molecular Target New Drug Study, Institute of Pharmacy & Pharmacology, Affiliated Nanhua Hospital, University of South China, 28 Western Changsheng Road, Hengyang 421001, Hunan, PR China. E-mail: yangzehua@usc.edu.cn, zhengxing9166@sohu.com
†These two authors contributed equally.

Shulei Wu

Shulei Wu was born in Hunan Province, China. She received her Bachelor's degree in the major of Pharmacy from the University of South China in 2020, and she is currently pursuing her Master's degree in the major of Pharmacy at the University of South China under the supervision of Dr Zehua Yang. Her research topic focuses on asymmetric catalysis.

Zaoduan Wu

Zaoduan Wu received his Master's Degree in clinical medicine from the University of South China in 2015 and then worked in the affiliated Nanhua hospital of the University of South China as a physician. Her scientific interests are in the area of bioactivity of new chemical entities.

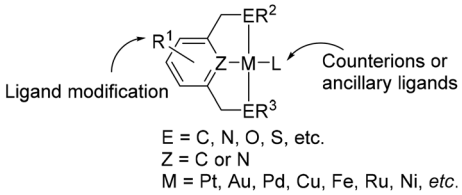

Fig. 1 Structural properties of pincer metal complexes.

of various functionalized auxiliary ligands. In addition, the different properties of the various metal centers seem to give them different pharmacological targets, which is expected to overcome cisplatin resistance. Therefore, the potential of pincer metal complexes as effective antitumor drugs has received widespread attention. However, most of the studies on pincer metal complexes are mainly focused on catalysis.[6] In recent years, although there have been reviews on the biological activity of metal coordinated compounds, these articles place emphasis on platinum, palladium, gold, copper and ruthenium,[7] while ignoring the potential of iron, nickel and other metals as antitumor agents. This review summarized the significant progress of the antitumor activity of pincer platinum(II), gold(III), palladium(II), copper(II), iron(III), ruthenium (II), nickel(II) and some other metal complexes.

2 Pincer Pt(II) complexes

The great success of cisplatin has stimulated worldwide efforts to develop new antitumor platinum-based complexes. The major challenges in the clinical application of cisplatin are its side effects and drug resistance.[3] A variety of platinum coordinated compounds have been investigated. Pincer Pt(II) complexes are attractive as novel antitumor drugs due to their excellent stability and rich chemical properties.

2.1 CNN-pincer Pt(II) complexes

The pincer Pt(II) complex [Pt^{II}(CNN)Cl] (**1**) (Fig. 2), where CNN = 6-phenyl-2,2′-bipyridyl, is structurally analogous to DNA intercalator [Pt^{II}(terpy)Cl]$^+$ (terpy = 2,2′:6′,2″-terpyridine). However, it was reported to be almost non-cytotoxic (IC_{50} > 236 μM).[8] More modifications are necessary. N-Heterocyclic carbene (NHC) ancillary ligands can improve the stability of metal coordination compounds and give them unique physical and chemical properties.[9] Complex [(CNN)Pt^{II}(NHC)]$^+$ (**2**) (Fig. 2) was found to display promising antitumor activity *in vitro* towards HeLa, HepG2, and SUNE1, and specifically displays the highest cytotoxic potency towards HeLa cells. The cytotoxicity against the NCI-H460 tumor of complex **2** at 3 mg kg^{-1} was comparable with cyclophosphamide at 30 mg kg^{-1} *in vivo* without apparent weight loss or death of mice.[10] Dinuclear complex **3** was also more effective than cisplatin, but less active than mononuclear complex **2**.[10]

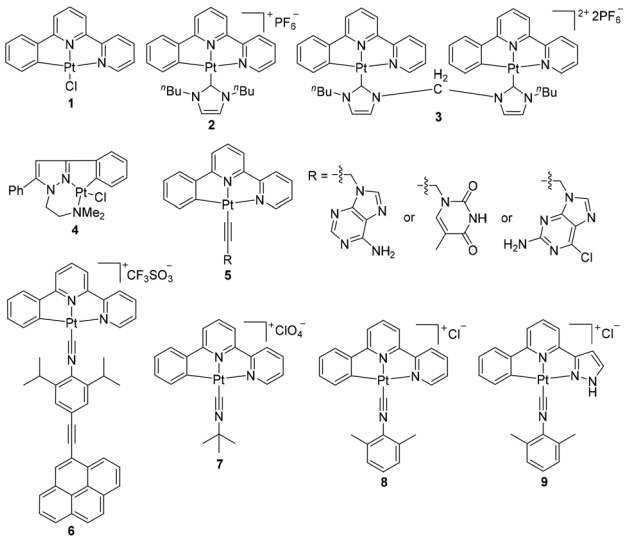

Fig. 2 CNN-pincer Pt(II) complexes as antitumor agents.

In the search of novel metal coordination compounds with potential antitumor activity, special attention has been paid to the replacement of one or both amino ligands of cisplatin by other N-donor ligands. Quirante *et al.*[11] developed platinum-based complex **4** with a C,$N_{pyrazole}$,N′-pincer ligand and evalu-

Qianyi Ge

Qianyi Ge was born in Hebei Province, China. She received her bachelor's degree in the major of pharmaceutical engineering from Weifang University, China, in 2019. She is currently pursuing her master's degree in the major of pharmacy at the University of South China under the supervision of Dr Zehua Yang. Her current research interests include organometallic chemistry as well as chiral ligand design and synthesis.

Xing Zheng

Xing Zheng received his Ph.D. in Chemistry from the Donghua University, China. He also worked as a postdoctoral fellow at Arizona State University and Wayne State University. He moved back to the University of South China where he was promoted to Professor in 2010. His scientific interests are in the areas of organofluorine chemistry, medicinal chemistry and natural product chemistry.

ated its cytotoxic activity *in vitro*. The obtained IC_{50} values indicated that the CNN tridentate Pt(II) complex was more effective than its Pd(II) analog and *N,N′*-bidentate Pt(II) complex. More modifications on the pyrazolyl and nitrogenous pendant arm open up a vast array of possibilities for the design of antitumor candidates.

Topoisomerase II (TopoII), which is closely related to DNA replication and transcription, is regarded as a potential target of antitumor drugs.[12] Che *et al.*[13] designed platinum(II) complexes $[(CNN)Pt^{II}(C{\equiv}CCH_2R)]$ (**5**) (Fig. 2) bearing acetylide ligands containing nucleobase motifs and evaluated their interaction with TopoII. The planar complexes intercalate into DNA and stabilize the TopoII-DNA cleavable complex. The MTT (3-(4,5-dimethylthiazol-2-yl)-2,5-diphenyltetrazolium bromide) assay suggests that they display better antitumor activities than cisplatin with IC_{50} = 0.8–10.7 μM upon 72 h of incubation in tested cancer cells *in vitro*.

Transcription factors are a class of proteins that control the flow of genetic information from DNA to mRNA. As tumor cells proliferate rapidly, transcription factors are overactive, which could be promising targets of antitumor drugs.[14] Che *et al.*[15] investigated the effects of the $[(CNN)Pt^{II}(C{\equiv}NL)]^+$ scaffold on the interaction of DNA and transcription factors. They found that complex **6** (Fig. 2) selectively bound to the DNA major groove and suppressed the DNA/CREB (cAMP response element binding protein) complex formation. The large π-surface auxiliary ligand plays an important role in conferring the mechanism to complex **6**. Although complex **6** only exhibited moderate cytotoxicity towards HeLa, HepG2 and SUNE1 cells with IC_{50} = 19.7–25.3 μM upon 72 h of incubation, it was almost non-cytotoxic against normal CCD-19Lu (IC_{50} > 100 μM).[15] The same group has found that cyclometalated platinum(II) complex **7** (Fig. 2) selectively inhibited TNF-α (tumor necrosis factor-α) stimulation of NF-κB (nuclear factor κB) gene transcription.[16] It also could stabilize the Topo I-DNA-**6** complex, resulting in DNA cleavage and cell apoptosis. The MTT assay results indicated that complex **7** displayed promising cytotoxicity against SUNE1 (IC_{50} = 0.13 μM) and NCI-H460 (IC_{50} = 0.11 μM) cells upon 72 h of incubation *in vitro*.[17]

Zehua Yang

Zehua Yang received his Ph.D. in Pharmacy from Shanghai Jiao Tong University, China, in 2015 and then worked in the University of South China as a lecturer. During this period, he also worked as a visiting scholar in Boston College, USA, for one year in 2020. His scientific interests are in the areas of asymmetric synthesis, organometallic chemistry, and medicinal chemistry.

Nano-formulation has been proved to enhance the stability and reduce the toxic side effects of antitumor drug candidates.[18] Che *et al.*[19] had reported $[Pt(CNN)(C{\equiv}NR)]^+$ (**8**) (Fig. 2), which self-assembled in water to form nanoaggregates. It accumulated in cancer cells and induced HeLa cell death (IC_{50} = 2.55 μM after 24 h of incubation). They also reported that Pt(II) complex **9** (Fig. 2) was pH-sensitive, which in acidic lysosomes accumulates and undergoes self-assembly. **9**-Hydrogel displayed a sustained release property at pH 7.4 and an acidic environment can stimulate a faster release of **9** from **9**-hydrogel and result in cytotoxicity towards different cancer cells, whose microenvironment is often acidic compared to that of normal tissues, achieving selective cytotoxicity towards cancer cells *in vivo*.[20]

2.2 CNC-pincer Pt(II) complexes

NHCs are considered to be excellent ligands for metal coordination compounds due to their electron-rich and easy modification.[9] Dinda and co-workers described that square planar complex **10** (Fig. 3) bearing a CNC-pincer carbene ligand displayed moderate cytotoxicity only to A549 cells (IC_{50} = 40 μM for 48 h treatment),[21] but almost non-cytotoxicity toward HCT116 and MCF-7 cell lines, which indicated that further modification was needed.

Garbe and co-workers prepared Pt(II) complexes **11–13** (Fig. 3) containing a CNC type pincer skeleton and DMSO or MeCN as neutral ligands. Complex **11b** displayed the most effective cytotoxicity against HT-29 and MDA-MB-231 cell lines. The cytotoxicity of these complexes was found to follow the trends below in the MTT assay (Table 1): (i) the cytotoxicity increases with lateral π system expansion; (ii) phenyl substituents on pyridine generally cause reduced cytotoxic activity; (iii)

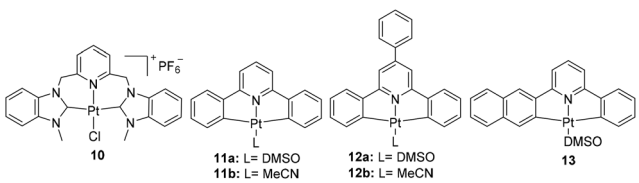

Fig. 3 CNC-pincer Pt(II) complexes as antitumor agents.

Table 1 IC_{50} values (μM) of CNC-pincer Pt(II) complexes (**11–13**) toward two human tumor cell lines[22]

Complex	IC_{50} value[a] (μM)	
	HT-29	MDA-MB-231
11a	16.44	12.12
11b	2.05	2.52
12a	11.88	8.68
12b	11.16	4.57
13	10.92	7.48

[a] Incubation for 72 h (HT-29) or 96 h (MDA-MB-231) at 37 °C with 5% CO_2.

Pt(CNC)MeCN complexes seem to be more effective than Pt(CNC)DMSO complexes.[22] Complex **12a** was found to hijack NF-κB protein as a carrier and subsequently transfer into the nucleus in tumor cells. Compared with clinical cisplatin, complex **12a** showed not only 9-fold higher toxicity towards HepG2 cells (IC_{50} = 0.28 μM for 48 h treatment), but also significantly reduced toxicity towards HELF (human normal embryonic lung fibroblasts). The tumor growth inhibition of complex **12a** in a mice model was also greater than that of cisplatin, and only slight inflammation was observed in kidney tissue sections of mice in the complex **12a** treated group.[23]

2.3 NCN-pincer Pt(II) complexes

Vezzu and co-workers found NCN-pincer Pt(II) complex **14a** (Fig. 4) with a chloride ligand displayed high cytotoxicity against tumor cells, while the cytotoxicity of the isomeric CNN-pincer Pt(II) complex was very low (IC_{50}, 24 h > 236 μM).[8] This apparent difference was attributed to the stronger trans effect of the carbon donor in **14a**, which makes the chloride ligand easier to dissociate and expose an active binding site to interact with DNA.[8] Complex **14b** (Fig. 4) exhibited 8 times more toxicity to HeLa cells than that under dark conditions when exposed to 405 nm light, which is a potential photosensitizer for photodynamic therapy. It was observed that complex **14b** mainly accumulated in the nucleus and induced irreversible DNA single-strand breaks upon irradiation with light. ROS/singlet oxygen ($^1O_2$) is involved in DNA damage.[24]

It is reported that the toxicity of Pt(II) complexes **15** (Fig. 4) containing NHCs against HeLa cells was much better than that of cisplatin.[25] Their 72 h cytotoxicity follows the order of **15c** (IC_{50} = 0.46 μM) > **15d** (IC_{50} = 1.70 μM) > **15a** (IC_{50} = 2.45 μM) > **15b** (IC_{50} = 3.00 μM), which is consistent with the improvement of lipophilicity. Interestingly, complex **15c** efficiently accumulated in the cytoplasm of tumor cells and induced mitochondrial dysfunction.[25]

The connection of antitumor drugs with targeting peptides through amide bonds to achieve targeted drug delivery has attracted the interest of researchers. Sarli *et al.*[26] prepared Pt complex **16** (Fig. 4) linked with a c(RGDyK) peptide. It is noteworthy that complex **16** showed enhanced growth inhibitory activity against the tested tumor cell lines for 48 h of incubation in the MTT assay, especially human breast MDA-MB-231cells (GI_{50} = 10 μM), compared to the Pt complex without the c(RGDyK) peptide (GI_{50} = 26 μM). The survival of rat bladder AY27 tumor cells incubated with complex **16** after 5 minutes of light exposure was significantly lower than that of the control group.[26]

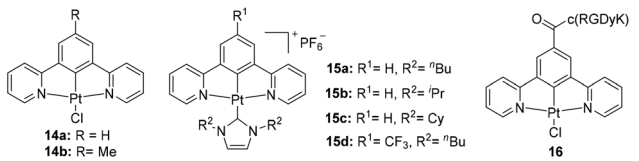

Fig. 4 NCN-pincer Pt(II) complexes as antitumor agents.

2.4 ENS-pincer Pt(II) complexes

The metal complexes of sulfur-nitrogen chelating agents have attracted interest because of their interesting physical and chemical properties and potential pharmacological properties. Given the significance of platinum(II) complexes in cancer chemotherapy, the antitumor activities of a series of Pt compounds with NNS tridentate ligands have been investigated. However, most of the NNS-Pt complexes did not show obviously increased cytotoxicity, and some even showed decreased or no cytotoxicity. For instance, Ali *et al.*[27] studied the cytotoxicity of two platinum(II) complexes (**17**) bearing tridentate NNS Schiff base ligands (Fig. 5). Unfortunately, only complex **17a** is moderately active against the human ovarian Caov-3 cancer cell line. Kovala-Demertzi *et al.*[28] found that Pt complex **18** (Fig. 5) only exhibited selectivity against A-549 and T24 cell lines, while the free thiosemicarbazone ligand showed strong cytotoxicity against MCF-7, A549, and T24 cell lines with IC_{50} = 3.04–11.80 μM after 72 h of incubation. Moreover, the survival time of the leukemia bearing mice treated with complex **18** was significantly increased compared to that with the ligand. The square-planar ONS pincer Pt(II) complex **19** displayed a maximum inhibition E_{max} of 72%, while its IC_{50} value was as high as 360-fold that of cisplatin upon 48 h of incubation.[29] The 4N-*ortho*chlorophenyl substituted thiosemicarbazone scaffold exhibited a high level of cytotoxicity to both MCF-7 and HT-29 cell lines at nanomolar doses. However, coordination with platinum(II) (**20**) did not show any obvious benefits but showed a selective inhibitory effect on thioredoxin reductase (TrxR), which is involved in numerous metabolic pathways and tumor development.[30] Recently, Rahman *et al.*[31] found that salicylaldimine based ONS pincer Pt(II) complexes **21** and **22** (Fig. 5) showed higher cytotoxicity than cisplatin in A549, HT-29 and MDA-MB-231 cells, and **22** with 4-picoline as the substituent was more active. It seems that they have an inhibitory effect on the invasion and migration of cancer cells, suggesting their potential in the field of aggressive tumor therapy.

3 Pincer Au(III) complexes

The pharmacological activity of gold complexes has been extensively studied since auranofin was used for the treatment

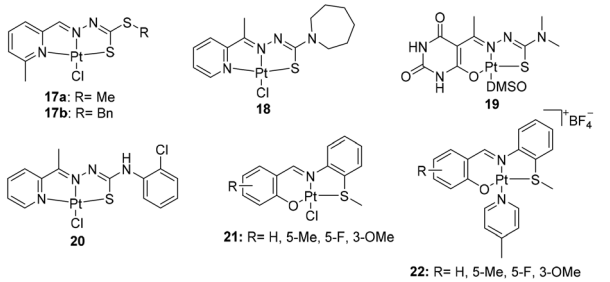

Fig. 5 ENS-pincer Pt(II) complexes as antitumor agents.

of rheumatoid arthritis. The antitumor properties of auranofin reported by Lorber[32] stimulated the research on gold complexes as potential antitumor drugs. Au(III) has a d^8 electronic configuration and is thus isoelectronic to platinum(II). However, it has been proposed that a variety of proteins inside cells are the primary targets of Au(III) complexes, which is distinct from general Pt(II) complexes.[33] Au(III) was easily reduced by thiols in the intracellular milieu which makes the choice of ligands very important.

3.1 NNN-pincer Au(III) complexes

Two types of gold(III) complexes (**23**, $[Au(dien)Cl]Cl_2$ (dien = diethylenetriamine); **24**, $[Au(terpy)Cl]Cl_2$) (Fig. 6) have been synthesized.[34] Cytotoxicity studies against the human ovarian A2780 cancer cell line show that diethylenetriamine is non-cytotoxic, while it coordinated with the gold(III) center to show potential toxicity (IC_{50} = 8.2 μM for 72 h), but whether terpyridine is coordinated with or without gold seems to have no effect on its cytotoxicity. This is because the properties of complex **23** are mainly from the NNN pincer-Au(III) itself, while those of complex **24** seem to come from the terpyridine ligand, which is in good agreement with the stability of the complexes in the presence of physiological reductants. Complex **24** seemed to be easily reduced and the terpyridine ligand was released, but complex **23** was stable in sodium ascorbate.[34a] Noteworthily, the binding affinity to calf thymus DNA of both **23** and **24** was electrostatic in nature and reversible.[34b] Further research studies proved that complex **23** formed tight metal–protein adducts with bovine serum albumin (BSA), which might account for biological effects.[34c]

The cytotoxicity of Au(III) complexes **25** and **26** (Fig. 6) was reported to increase with increasing lipophilicity (Table 2). In the presence of glutathione (GSH), they are quickly reduced and release Au(I)-NHC complexes, which are responsible for their antitumor effects. They mainly accumulate in the cytoplasm and TrxR is a possible biomolecular target.[35] Nevertheless, complexes **27** and **28** (Fig. 6) were remarkably stable under a physiological-like environment. Due to the poor solubility of complex **27b** and **28** in the cell culture medium, only the cytotoxicity of complex **27a** was studied. Complex **27a** showed higher cytotoxicity than cisplatin towards the three tested tumor cells with IC_{50} = 11–20 μM upon 48 h of incubation.[36]

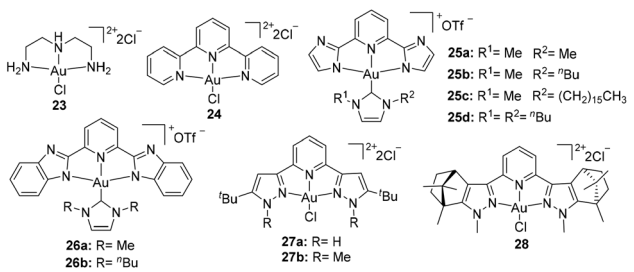

Fig. 6 NNN-pincer Au(III) complexes as antitumor agents.

Table 2 IC_{50} values (μM) of NNN-pincer Au(III) complexes (**25** and **26**) toward four human tumor cell lines[35]

	IC_{50} value[a] (μM)			
Complex	HeLa	HepG2	NCI-H460	MCF-7
25a	32.9	36.2	55.0	18.4
25b	16.5	33.2	11.0	17.2
25c	1.4	3.3	1.4	2.9
25d	13.0	28.7	7.9	12.9
26a	14.4	18.0	11.2	11.9
26b	9.2	14.7	5.5	8.7

[a] Incubation for 72 h at 37 °C with 5% CO_2.

3.2 CNN-pincer Au(III) complexes

Messori and co-workers reported that Au(III) complex **29a** (Fig. 7) exhibited promising cytotoxic properties toward the tested tumor cells[37] and interacted tightly with TrxR,[38] cytochrome *c* and lysozyme.[39] It also formed tight derivatives with the copper chaperone Atox-1, which was crucial to the copper transfer and delivery system. This suggested complex **29a** might enter the cells through the copper trafficking system.[40] 87 differently expressed proteins were up-regulated or down-regulated by treating with complex **29a**, which might perturb mitochondrial processes and the glycolytic pathway.[41]

To confirm if the replacement of the hydroxyl ligand might influence the pharmacological properties of **29a**, the toxic activities of **29b** and **29c** (Fig. 7) against human tumour cell lines were tested. Both of them exhibited enhanced bioactivity in comparison to **29a** (Table 3), while they seemed to work by hydrolysis and releasing the parent hydroxo-complex.[42] The mean IC_{50} value of dinuclear oxo-bridged complex **30** (Fig. 7) in the tested cells is 24.51 μM upon 72 h of incubation, which is not significantly different from mononuclear complex **29a** (27.71 μM). The oxygen bridge fractured and gave two mononuclear species responsible for its toxic properties.[43]

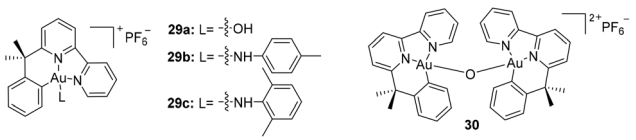

Fig. 7 CNN-pincer Au(III) complexes as antitumor agents.

Table 3 IC_{50} values (μM) of CNN-pincer Au(III) complexes (**29**) toward three human tumor cell lines[42]

	IC_{50} value[a] (μM)		
Complex	A2780/S	A2780/R	MCF-7
29a	8.20	12.70	35.30
29b	6.15	14.30	18.10
29c	2.50	5.70	5.20

[a] Incubation for 72 h at 37 °C with 5% CO_2.

3.3 CNC-pincer Au(III) complexes

It has been reported that Au^{III}(CNC)L complex **31** (Fig. 8) based on the 2,6-diphenylpyridine ligand was found to be toxic against HeLa, HepG2, SUNE1 (cisplatin-sensitive), and CNE1 (cisplatin-resistant) cell lines,[44] whereas complexes **32** (Fig. 8) obtained by replacing chlorine with several substituents showed higher IC_{50} values. Dinuclear complexes **33** (Fig. 8) with a diphenylphosphine linker also exhibited extraordinary cytotoxicity and complex **33c** was most cytotoxic (Table 4). Shortening or lengthening the hydrocarbon linker would reduce its activity.[44]

CNC-pincer Au(III) complex **34** (Fig. 8) with an NHC as an auxiliary ligand displayed much higher antitumor properties than cisplatin *in vitro* and inhibited tumor growth in nude mice without any weight loss or death, while dinuclear complexes **35** (Fig. 8) did not exhibit any improvement in activity (Table 5).[45] The cytotoxicity of type **34** complexes was observed to improve with the increase of the alkyl chain length of the NHC ligand. To further investigate its molecular targets, Che *et al.*[46] prepared probe **36** (Fig. 8). When exposed to light, it could form covalent bonds with six binding proteins in cells, which were described as potential antitumor targets.

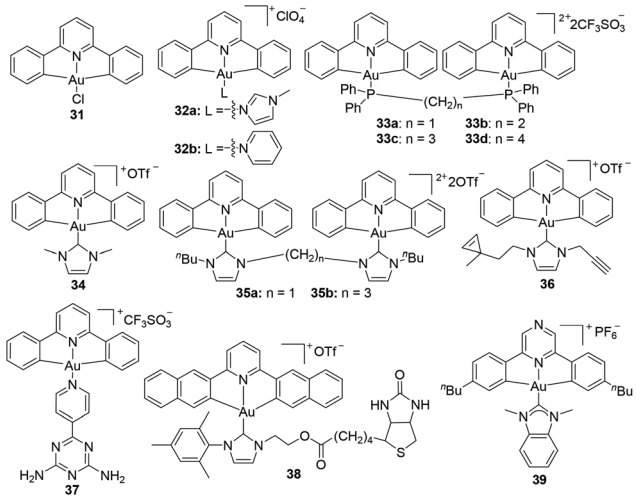

Fig. 8 CNC-pincer Au(III) complexes as antitumor agents.

Table 4 IC_{50} values (μM) of gold complexes (**31–33**) toward four human tumor cell lines[44]

	IC_{50} value[a] (μM)			
Complex	HeLa	HepG2	SUNE1	CNE1
31	3.4	17	4.0	3.1
32a	8.0	35	12	6.7
32b	8.2	84	4.0	2.6
33a	0.81	n.d.	0.92	1.2
33b	0.14	0.32	0.25	0.40
33c	0.04	0.21	0.05	0.09
33d	2.4	n.d.	1.5	2.2

[a] Incubation for 72 h at 37 °C with 5% CO_2; n.d. = not determined.

Table 5 IC_{50} values (μM) of the CNC-pincer Au(III) complexes (**34** and **35**) toward three human tumor cell lines and the normal lung fibroblast cell line[45]

	IC_{50} value[a] (μM)			
Complex	HepG2	SUNE1	NCI-H460	CCD-19Lu
34	0.37	0.25	0.17	25
35a	7.9	3.3	3.0	>100
35b	1.1	3.0	1.2	16

[a] Incubation for 72 h at 37 °C with 5% CO_2.

Che *et al.*[47] also reported the use of self-assembled pincer-Au(III) complex **37** (Fig. 8) in cancer treatment, which exhibited a sustained toxic effect on melanoma B16 cells. Studies on complex **37** showed that it could release the anti-angiogenic 2,4-diamino-6-(4-pyridyl)-1,3,5-triazine ligand sustainably and form an adduct with GSH under physiological conditions. Complex **38** (Fig. 8) obtained by coupling a biotin scaffold with a pincer gold complex displayed promising cytotoxicity towards HeLa, HepG2 and MDA-MB-231 cancer cell lines with IC_{50} values (48 h) ranging from 1.2 to 2.8 μM.[48] It was observed that complex **39** (Fig. 8) showed remarkable toxicity toward HL60 and MCF-7 cells with IC_{50} values (72 h) down to nanomolar levels ranging from 0.31 to 0.56 μM. Complex **39** also showed potent effects even for the highly drug-resistant A549 cell line (IC_{50} = 7.8 μM).[49]

4 Pincer Pd(II) complexes

Palladium complexes have been candidates for metal coordinated antitumor drugs because of their similarities of structural and thermodynamic properties to platinum complexes. However, the rate of the ligand exchange reaction under physiological conditions of palladium(II) complexes is much faster than that of platinum(II) complexes, resulting in the deactivation of palladium(II) complexes. The introduction of the pincer ligand can effectively improve their stability.

4.1 NNN-pincer Pd(II) complexes

Yilmaz *et al.*[50] firstly reported several palladium(II) and platinum(II) complexes of saccharin with bis(2-pyridylmethyl) amine as the pincer ligand. The complexes coordinated with platinum(II) are inactive, while palladium complexes **40** (Fig. 9)

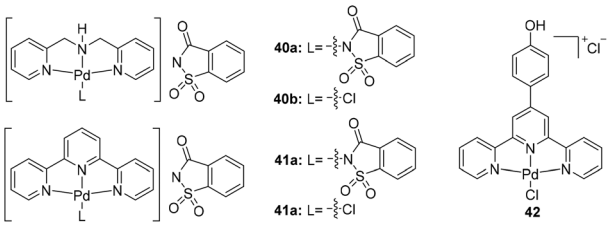

Fig. 9 NNN-pincer Pd(II) complexes as antitumor agents.

show high activity, especially to A549 cells (IC_{50}, 72 h = 23 μM), which is comparable to cisplatin (IC_{50}, 72 h = 20 μM). Complex **40b** was found to display promising anti-proliferative activity against MCF-7 and MDA-MB-231 cell lines with IC_{50} values (72 h) as low as 3.9 and 4.2 μM, respectively.[51]

Taking into account the promising activity of complex **40b**, palladium complexes **41** (Fig. 9) with 2,2′:6′,2″-terpyridine as the pincer ligand were synthesized and investigated.[52] Both of them significantly inhibited the proliferation of lung cancer cells, especially A549 cells (IC_{50} = 2.1–2.3 μM for 72 h treatment). Surprisingly, the formation of tubules of MDA-MB-231 human breast cancer cells treated with complex **41a** was disrupted, which indicated that complex **41a** had strong anti-invasive activity.[52a] Moreover, complex **41a** is less toxic to the liver, without significant changes in alanine aminotransferase (ALT) and aspartate aminotransferase (AST) levels.[52f] Therefore, complex **41a** can be considered as a potential antitumor chemotherapeutic drug with fewer hepatotoxic complications.

Complex **41b** was observed to possess broad antiproliferative activity against tumor cell lines with IC_{50} values (72 h) ranging from 1.41 to 21.7 μM.[52e] The mechanism of its antitumor activity is related to the type of tumor cells. Necrosis seems to be its main way to induce the death of non-small cell lung cancer cells.[52b] However, it seems to induce fibrosarcoma cell death in an apoptotic manner.[52c] There are also different mechanisms in breast cancer cells. Complex **41b** caused breast MDA-MB-435 cancer cell apoptosis not depending on the caspase-3 pathway,[52e] while the apoptosis of MCF-7 and MDA-MB-231 cells was through a caspase-dependent pathway.[52d]

Shahpiri *et al.*[53] reported the antiproliferative activity of complex **42** (Fig. 9) with a derivative of the terpyridine NNN pincer ligand against various human tumor cells. An obvious improvement in activity was observed compared with the free ligand, and its IC_{50} values against MCF-7, A-549, K562, and HT-29 cells were significantly lower than that of cisplatin. It is interesting that complex **42** interacts with DNA through a mixed-binding mode, involving covalent, intercalation and hydrogen-bonds.

4.2 CNN-pincer Pd(II) complexes

A unique palladium-based complex **43** (Fig. 10) *via* cyclopalladation of 2-arylphenanthroline was reported by Higgins III and co-workers.[54] Studies on **43** have displayed growth inhibition activity against a panel of six human cancer cell lines *in vitro* with IC_{50} values as low as 5–8 μg ml^{-1}. It possessed potent DNA binding activity, which was thought to be responsible for its antitumor effect.

α-Diimine has recently attracted widespread attention due to its versatile coordination performance. Its flexible E═C–C═N (E═O, N) bond skeleton displays excellent electron donor and acceptor properties.[55] Cruz *et al.*[56] have focused attention on the corresponding Pd-based compounds **44** (Fig. 10) with α-diimines as promising carrier ligands. It was expected that their antitumor properties could be modified systematically by varying the functional groups. Complex **44b** provides better results than complex **44a** against U251 and K562 cancer cells (IC_{50}, 48 h = 19.8 and 22.5 μM for **44b** compared with 23.6 and 25.4 μM for **44a**, respectively).

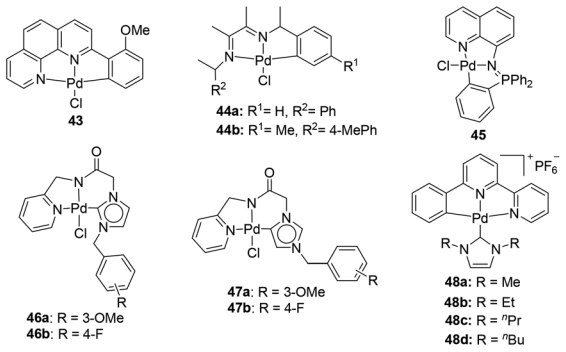

Fig. 10 CNN-pincer Pd(II) complexes as antitumor agents.

It has been reported that iminophosphorane and derivatives serve as stabilizing chelating ligands in antitumor metal coordinated compounds.[57] Frik *et al.*[58] synthesized a series of metal-based complexes with an iminophosphorane ligand and evaluated their antiproliferative properties. The new species with iminophosphorane acts as a CNN-pincer ligand were more stable and showed half-lives of several weeks in d^6-DMSO solution. They exhibited important cytotoxic effects in the low micromolar range in a human ovarian cancer cell line, especially Pd compound **45** (Fig. 10) was selective for A2780s. Studies revealed that compound **45** has almost no interaction with plasmid (pBR322) DNA, supporting the idea of different mechanisms of action with respect to cisplatin.

In order to slow down the rate of dissociation or hydrolysis of palladium(II) complexes, Lee *et al.*[59] designed an isomeric pair of palladium(II) complexes (**46** and **47**) bearing CNN tridentate ligands (Fig. 10). It was found that the anticancer activity of these complexes was highly structurally dependent. nNHC complex **46a** appeared to show activity superior to that of its isomeric aNHC complex **47a**. In contrast, replacing the *N*-3-methoxy group with an *N*-4-fluorobenzyl group led to higher activity of aNHC complex **47b** than nNHC complex **46b** toward human ovarian TOV21G cells (Table 6).

A new series of palladium(II) complexes **48** (Fig. 10) that introduced a strong σ-donor NHC auxiliary ligand were reported to be stable in the presence of biological thiols.[60]

Table 6 IC_{50} values of CNN-pincer Pd(II) complexes (**46** and **47**) toward three human cell lines[59]

	IC_{50} value[a] (μM)		
Complex	TOV21G	SW620	NCI-H1688
46a	6.05	46.13	211.0
46b	49.55	83.47	302.0
47a	—	79.2	248.0
47b	17.78	359.0	3351.0

[a] Incubation for 48 h at 37 °C with 5% CO_2.

Table 7 IC_{50} values of the CNN-pincer Pd(II) complexes (**48**) toward five human tumor cell lines[60]

	IC_{50} value[a] (μM)				
Complex	NCI-H460	MDA-MB-231	HeLa	A2780/R	A2780/S
48a	2.1	0.9	1.8	2.2	1.7
48b	1.1	0.9	1.4	1.8	1.5
48c	0.4	0.8	0.5	1.2	1.6
48d	0.08	0.5	0.1	0.5	0.2

[a] Incubation for 72 h at 37 °C with 5% CO_2.

They all exhibited superior toxicity against tested HeLa, NCI-H460, MDA-MB-231, A2780/S, and A2780/R tumor cell lines (Table 7), especially complex **48d** is 118-fold more toxic to NCI-H460 cells than cisplatin *in vitro* and their toxicity to normal cells is significantly reduced. Biochemical assays showed that complex **48d** caused apoptosis by inducing mitochondrial dysfunction and inhibiting the EGFR signal pathway, which suggests that complex **48d** is expected to be a potential agent against cisplatin-resistant tumor cells.[60]

4.3 NNS-pincer Pd(II) complexes

Guo and co-workers synthesized NNS-pincer Pd(II) complex **49** (Fig. 11) based on the 8-aminoquinoline derivative of L-methionine. Complex **49** containing a Pd–S bond exhibited higher cytotoxicity than the complex containing an L-alanine derivative against a series of cancer cell lines. The IC_{50} value (48 h) of complex **49** (10.4 μM) for the HeLa cell line was much lower than that of cisplatin (42.6 μM).[61] Kovala-Demertzi *et al.*[62] investigated the antiproliferative activity of coordination complex **50** (Fig. 11) based on the 2-formylpyridine-4-*N*-ethyl-thio-semicarbazone ligand. The free ligand displayed comparable activity to cisplatin against MCF-7 and T-24. When it coordinated with Pd(II), its cytotoxicity against T-24 cells enhanced, becoming 7 times better than that of cisplatin, which can be regarded as a promising antitumor agent.

Pincer-type palladium(II) complexes derived from *N*-picolinylamides functionalized with *S*-methyl-cysteine (**51**) and methionine (**52**) (Fig. 11) were tested for cytotoxicity against cancer HCT116, MCF-7, PC3 and normal HEK293 cell lines. MTT assay results demonstrated that almost all NNS-Pd (II) complexes containing an S-donor displayed higher cytotoxic

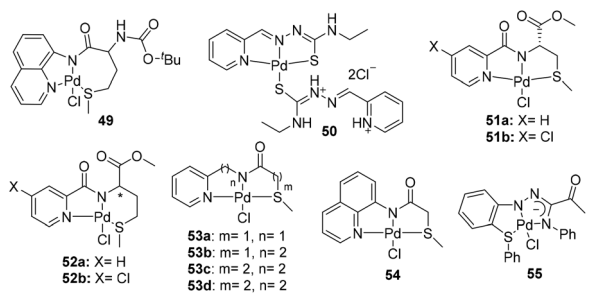

Fig. 11 NNS-pincer Pd(II) complexes as antitumor agents.

Table 8 IC_{50} values of the NNS-pincer Pd(II) complexes (**51** and **52**) toward four human cell lines[63]

	IC_{50} value[a] (μM)			
Complex	HCT116	MCF-7	PC3	HEK293
51a	1.8	22.0	>30	18.0
51b	1.2	10.0	16.5	8.0
(***S***)**-52a**	6.2	15.5	13.5	16.5
(***S***)**-52b**	0.45	5.5	4.2	4.0
(***R***)**-52a**	7.0	15.0	8.5	16.2
(***R***)**-52b**	4.4	11.7	4.5	11.0

[a] Incubation for 48 h at 37 °C with 5% CO_2.

activity than cisplatin with IC_{50} values (48 h) from 0.45 to 16.5 μM (Table 8), but the NNN-Pd(II) complexes derived from histidine containing an N-donor even promoted the growth of tumor cells, which indicated that the presence of an S-donor group was crucial for the cytotoxicity of this type of palladium (II) complex. Moreover, the chlorine substituent on the pyridine ring of NNS complexes increased the cytotoxic activity.[63]

Encouraged by the effective cytotoxicity of complexes **51** and **52**, the same group also evaluated the antiproliferative potential of pincer Pd(II) complexes **53** and **54** based on functionalized carboxamides (Fig. 11). Almost all sulfide-based 5,5- and 5,6-membered complexes exhibited a high level of cytotoxicity against HCT116 and PC3 cancer cell lines (Table 9). Their corresponding sulfoxide derivatives appeared to be less active or even non-cytotoxic.[64] However, the antitumor activity of the complexes obtained in this study is not as good as that of the previously reported NNS-pincer complexes **51** and **52** bearing amino acid pendant arms.

Palladium(II) complex **55** derived from an SNN amidrazone pincer ligand (Fig. 11) interfered with tumour growth by inhibiting the levels of vascular endothelial growth factor (VEGF) expression. Moreover, complex **55** exhibited much more activity on two breast cancer cell lines (MCF-7 and T47D) and less toxicity against normal Vero cells (IC_{50}, 48 h = 147.9 and 138.2 μM for MCF-7 and T47D compared with 611.09 μM for Vero, respectively). The increased level of caspase-3 activity suggests that apoptosis is the manner of complex **55** to induce cancer cell apoptosis.[65]

Table 9 IC_{50} values of the NNS-pincer Pd(II) complexes (**53** and **54**) toward four human cell lines[64]

	IC_{50} value[a] (μM)			
Complex	HCT116	MCF-7	PC3	HEK293
53a	12	40	17	14
53b	17	26	26	18
53c	12.5	32	20	16
53d	60	>100	82	74
54	19.5	42	20	7

[a] Incubation for 48 h at 37 °C with 5% CO_2.

4.4 ONS-pincer Pd(II) complexes

When oxygen is added as the third donor site to the NS bidentate thiosemicarbazone ligands, the binding mode of thiosemicarbazones will be changed to ONS coordination. The thiosemicarbazones coordinate with palladium(II) as tridentate ONS pincer donors to form stable 5,6-membered cyclic-palladium complexes **56** (Fig. 12). It was found that **56** interacted with CT-DNA in the electrostatic (**53b** and **53c**) or intercalative (**56a** and **56d**) mode. Their antitumor activity in A549 and HepG2 cells followed the order of **56c** > **56b** > **56a** ≈ **56d**.[66] Natarajan *et al.*[67] demonstrated that palladium compound **57** (Fig. 12) coordinated in a tridentate ONS manner is more cytotoxic against HeLa, HEp-2 and HepG2 cells than palladium compounds coordinated in a bidentate NS manner. They also found that in palladium compound **58** (Fig. 12) with the same ONS donor thiosemicarbazone ligand, triphenylarsenic at the fourth ligand site was more potent than triphenylphosphine.[68] The biological properties of palladium(II) complexes **59** (Fig. 12) containing SNO pincer *N*-substituted isatin thiosemicarbazones have been evaluated. All three compounds exhibited non-covalent binding to DNA. They possess significant anti-proliferative activity against MCF-7 and A549 cells after 24 h of incubation, with an IC_{50} value of ~22.92 μM.[69] Among the salicylaldimine palladium compounds reported by Zhang *et al.*, it was found that methionine based ONS palladium compound **60** (Fig. 12) can arrest cell cycles in A549 cells and effectively inhibited cell growth.[70]

5 Pincer Cu(II) complexes

Copper is a crucial transition metal involved in various biological processes in living organisms. Taking this into account, the development of copper complexes in the treatment of diseases has attracted great attention.

5.1 Cu(II) complexes with ONN donor sets

It is well known that copper(II) and its complexes are effective "chemical nucleases", which can induce DNA hydrolysis or oxidative cleavage in the presence or absence of external reagents. DNA is an important biological target for antitumor drugs. Therefore, copper(II) complexes have been proposed as promising cytotoxic agents. Square-planar Cu(II) complex **61** (Fig. 13) unexpectedly cleaved supercoiled double-stranded DNA without adding any reducing agents. The addition of a hydroxyl scavenger can effectively inhibit the cleavage activity of **61**, which proves that it interacts with DNA through oxidative cleavage, and the hydroxyl radical is its active substance.[71] Complex **62** (Fig. 13), a square pyramidal monomeric molecule, cleaves DNA involving ROS such as a hydroxyl radical, $^1O_2$ and hydrogen peroxide. Its IC_{50} values (48 h) were determined to be 16.123 μM and 9.8 μM against HeLa and MCF-7 cell lines, respectively.[72] Potential molecular mechanism research studies suggested that **62** induced the intrinsic mitochondrial apoptosis pathway due to the activation of caspase-9 and caspase-3.[72a]

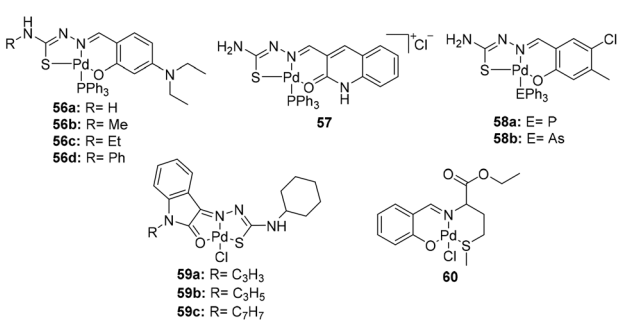

Fig. 12 ONS-pincer Pd(II) complexes as antitumor agents.

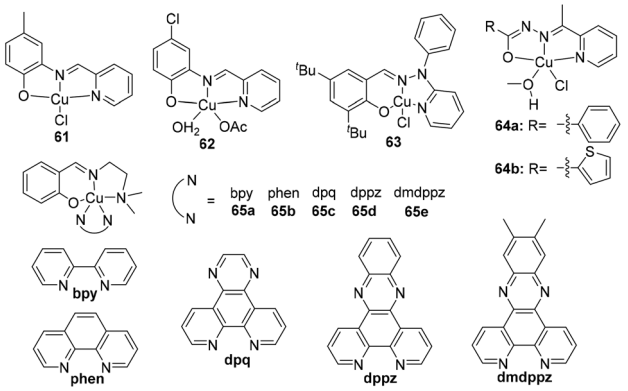

Fig. 13 Cu(II) complexes with ONN donor sets as antitumor agents.

Mandal *et al.*[73] prepared complex **63** (Fig. 13) that could cleave plasmid DNA *via* self-activation. The addition of NaN_3 and L-histidine significantly inhibited nuclease activity, proving that $^1O_2$ species participated in the oxidative cleavage of DNA. Antitumor activity studies confirmed that complex **63** has excellent cytotoxicity towards MCF-7 cells with IC_{50}, 96 h = 4.76 μM, while the IC_{50} value of cisplatin under the same experimental conditions is 17.98 μM. Complexes **64** (Fig. 13) synthesized by Dharmaraj can not only interact with DNA through intercalation, but also cleave supercoiled pBR322 DNA without adding any reducing agents.[74] The authors observed that DNA cleavage seemed to follow a mechanism of hydrolysis that does not involve free radicals, because the addition of free radical scavengers or the presence or absence of oxygen has no effect on activity. There is no difference between their cytotoxicity against HeLa cells. Their toxicity against various tested tumor cells *in vitro* is 6–43 times as high as that of cisplatin, while both of them have a low antiproliferative effect on normal NIH 3 T3 cells and are considered as excellent candidates for emerging antitumor drugs.[74]

To further study the effect of auxiliary ligands on the properties of ONN-pincer copper complexes, a series of complexes **65** (Fig. 13) with diimine (NN) co-ligands have been tested for DNA cleavage and antitumor activities.[75] All complexes exhibited effective DNA cleavage activity without adding any reducing agents. Adding DMSO, glycerol and methanol or anaero-

bic conditions did not significantly inhibit the efficiency of the complex, which excludes the mechanism involving hydroxyl radicals (˙OH) and active oxygen. Based on these findings, the cytotoxicity of **65** against MCF-7 and ME180 was examined. Their cytotoxic activity follows the order of **65d** > **65e** > **65c** > **65b** > **65a** (Table 10), which is consistent with the ability of DNA cleavage, and even the cytotoxicity of **65d** against MCF-7 cells for 24 hours of incubation is nearly 100 times that of cisplatin, which is promising to be further studied.[75]

5.2 NNN-pincer Cu(II) complexes

Hitherto, a large number of metal complexes with polypyridine as coordinated ligands have shown promising antitumor activity. Chao *et al.*[76] prepared three new terpy-copper(II) complexes **66** (Fig. 14), and investigated their interaction with DNA as well as their killing effects on HeLa, HepG2 and BEL-7402 tumor cell lines. The affinity of complexes **66** to DNA followed the order **66b** > **66a** > **66c**. They displayed effective DNA oxidative cleavage in the presence of glutathione, with hydrogen peroxide playing an important role in the cleavage reaction. According to MTT assay results, they all showed higher cytotoxicity than cisplatin against the tested cell lines with IC_{50} values (48 h) in the range of 2.72 to 8.98 μM. Interestingly, the cytotoxicity order of the complexes was not consistent with DNA affinity (Table 11). To explain this phenomenon, the authors further explored the biochemical mechanism of cytotoxicity. After treatment with these complexes, the level of ROS in the HeLa cells increased significantly, and the amount of reactive oxygen generation followed the order of **66c** > **66a** > **66b**, which is consistent with the IC_{50} values. Therefore, it is suggested that oxidative stress is the main mechanism by which complexes induce apoptosis.[76]

The choice of the coordination ligand is extremely important for the properties of metal complexes. The differences in the cytotoxicity of six copper(II) complexes derived from 2,2′:6′,2″-terpyridine (**67**) and 2,6-di(thiazol-2-yl) pyridine (**68**) (Fig. 14) were investigated.[77] Interestingly, it was observed that complexes **68** showed specificity towards A2780 cells, especially complex **68c** was >27 times more cytotoxic to A2780 cells than to other cancer cells. Among the terpy-Cu(II) complexes, **67a** is specific towards A2780 cells, and **67b** prefers HCT116 and A549 cells, while **67c** did not exhibit any cytotoxic activity (Table 12). The specificity of these complexes for different types of cancer cell lines is a property for further study.

To determine whether the number of copper centers will affect the properties, Vilar *et al.*[78] synthesized mononuclear (**69**), binuclear (**70**), and trinuclear (**71**) copper(II)-terpyridine complexes (Fig. 14) and investigated their antiproliferative activities against tumor cells. These complexes seem to interact with DNA through a mixed mode of intercalation and groove binding, of which planar terpyridine intercalates into DNA, and piperidine or copper(II)-bis(2-pyridylmethyl)arms interact with the groove. As the number of copper centers increases, the DNA cleavage activity of the complexes also gradually enhanced, and superoxide is the major ROS that induces DNA cleavage. Trinuclear complex **71** showed the highest antiproliferative activity, especially to the cisplatin-resistant MOLT-4 leukaemia cell line with IC_{50} = 23 μM upon

Table 10 IC_{50} values (μM) of the Cu(II) complexes (**65**) with ONN donor sets toward two human tumor cell lines[75]

	IC_{50} value[a] (μM)	
Complex	MCF-7	ME-180
65a	20.0	38.0
65b	2.00	28.6
65c	1.58	19.5
65d	0.46	17.0
65e	0.65	17.7

[a] Incubation for 24 h at 37 °C with 5% CO_2.

Table 11 IC_{50} values (μM) of the NNN-pincer Cu(II) complexes (**66**) toward three human tumor cell lines[76]

	IC_{50} value[a] (μM)		
Complex	HeLa	HepG2	BEL-7402
66a	5.34	2.72	5.32
66b	8.98	4.13	8.35
66c	3.03	3.91	6.21

[a] Incubation for 48 h at 37 °C with 5% CO_2.

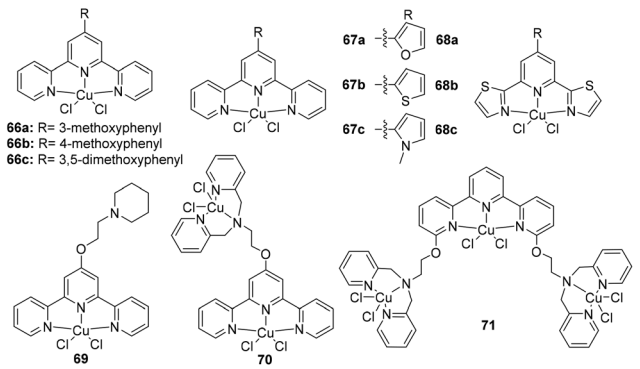

Fig. 14 NNN-pincer Cu(II) complexes as antitumor agents.

Table 12 IC_{50} values (μM) of the NNN-pincer Cu(II) complexes (**67** and **68**) toward four human tumor cell lines[77]

	IC_{50} value[a] (μM)			
Complex	HCT116	A2780	A549	MCF-7
67a	17.3	2.9	20.5	43
67b	2.1	>100	4.2	>100
67c	>100	>100	>100	>100
68a	81.7	5.9	64.3	>100
68b	20.5	4.6	22.6	62.3
68c	>100	2.6	70.1	89

[a] Incubation for 48 h at 37 °C with 5% CO_2.

24 h of incubation. Cell uptake studies showed that complex **71** accumulated in the nucleus, suggesting that it induced apoptosis by causing DNA damage and cell cycle arrest.

5.3 ONS-pincer Cu(II) complexes

The thiosemicarbazone derivatives undergo thione–thiol tautomerism in solution. The deprotonation of sulfur in the main thiol form turns the thiosemicarbazide into an anionic ligand that can coordinate with the metal cation. The biological activity of complexes **72–74** (Fig. 15) derived from *N*-substituted thiosemicarbazone was investigated.[79] The MTT assay revealed that square pyramidal complexes **72** were nearly noncytotoxic, while complexes **73** and **74** which coordinated with methanol exhibited potential cytotoxicity towards HeLa and NIH 3 T3 cells with IC_{50} values (48 h) of 10.6–39.3 μM, even though complex **73** also had square pyramidal geometry. The high cytotoxicity of complex **74** may be due to the fact that the presence of phenyl substitution changes the coordination mode of thiosemicarbazone, making complex **74** become square planar.[79] Binuclear copper complex **75** (Fig. 15) exhibited selective cytotoxicity against HeLa cells with IC_{50}, 48 h = 13.12 μM, while its IC_{50} values towards HepG2 and HEp-2 cells were determined to be >100 μM. It was observed that complex **75** strongly binds to DNA and BSA, and it induces DNA cleavage by hydrolysis not involving ROS.[80]

Gudasi *et al.*[81] used thiosemicarbazide of ethyl pyruvate (EP) derivatives to coordinate with Co(II), Ni(II), Cu(II) and Zn(II), and evaluated their anti-proliferative effects on K562 and COLO-205 cells. Copper complex **76** (Fig. 15) shows the highest cytotoxicity with IC_{50} values (48 h) of 8.65–15.16 μM against tested cell lines, while ligands and other complexes are biochemically inactive. The toxicity mechanism of complex **76** was further studied in COLO-205 cells. No significant increase of ROS generation in cells was observed after treatment with **76**, while sub-G_0/G_1 cell accumulation, DNA fragmentation, caspase-3 activation, and nuclear concentration were observed, suggesting that complex **76** caused cell death through a caspase dependent intrinsic mitochondria mediated apoptotic pathway.

6 Pincer Fe(III) complexes

Iron is the primary component of cytochrome proteins that regulate redox reactions in organisms. As a bio-essential metal for the human body, it is expected to be suitably designed as a novel antitumor agent with fewer metal-induced cell side effects.

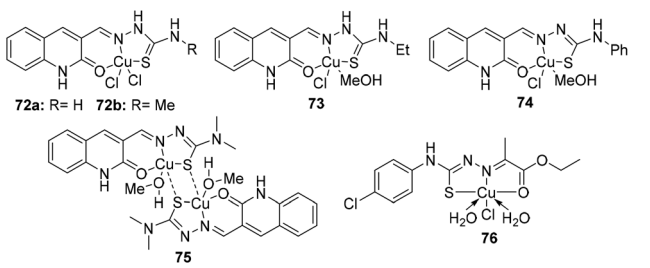

Fig. 15 ONS-pincer Cu(II) complexes as antitumor agents.

6.1 Fe(III) complexes with NEN tridentate ligands

Tridentate ligands derived from polypyridines seem to be a good option for the stabilization of metal complexes with potential cytotoxic properties. In view of the low inherent toxicity of iron, Gaiddon and Le Lagadec prepared an NCN monoanionic pincer iron complex **77** (Fig. 16).[82] The IC_{50} values (48 h) of complex **77** in human colon HCT-15 (0.2 μM), lung SKLU-1 (0.5 μM) and gastric AGS (0.7 μM), KATO III (0.8 μM) cancer cell lines proved that its activity was much higher than that of cisplatin. It caused cell death through a pathway involving ER stress and autophagy, rather than a caspase-dependent pathway.[82]

Photodynamic therapy (PDT) is a non-invasive mode of therapeutic treatment of cancer. The photosensitizer (PS) is the most important factor affecting the efficacy of PDT. A near-infrared (NIR) light PS provides better tissue penetration for further treatment of lung, breast, or liver cancer. Biocompatible iron complexes with versatile coordination geo-

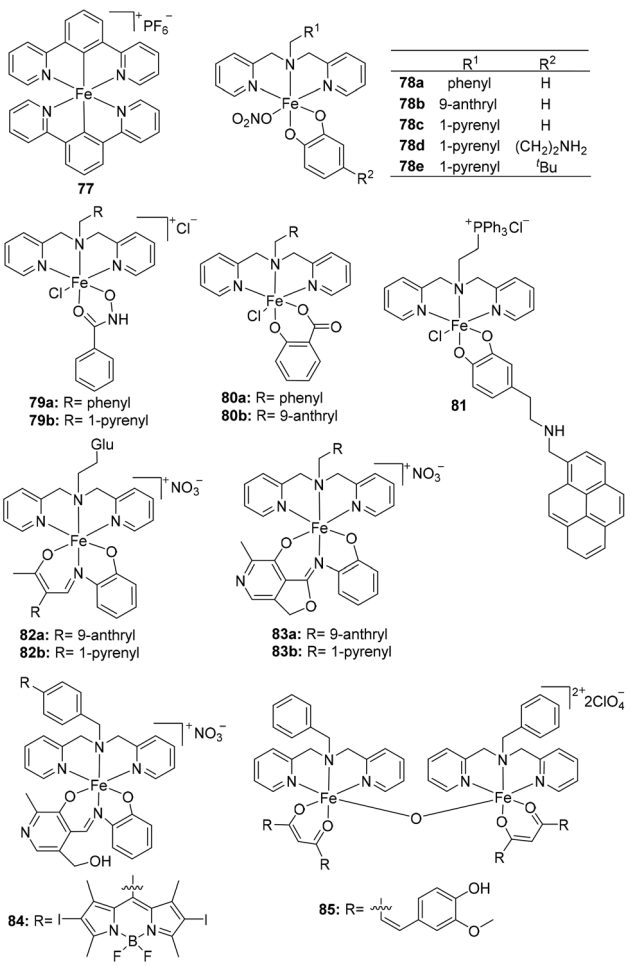

Fig. 16 Fe(III) complexes with NEN tridentate ligands as antitumor agents.

metries and redox properties could be reasonably designed as potent PDT agents. Chakravarty first synthesized ternary iron(III) complexes **78** (Fig. 16), which combined a planar phenyl/anthryl/pyrenyl modified dipicolylamine ligand as a PS-cum-DNA binder and a catecholate ligand for an NIR intense absorption band.[83] Complex **78a** did not show any apparent photocytotoxicity with IC_{50} values even >100 μM either irradiated with light or not. Complexes **78b–78e** with a planar anthryl or pyrenyl moiety were effective against cancerous HeLa, MCF-7, and A549 cells under NIR light irradiation (600–720 nm).[83b]

Replacing catecholate with a hydroxamate ligand (**79**) (Fig. 16) did not seem to be beneficial for photocytotoxicity against HeLa cells. However, it was unexpected to observe mitochondrial localization of **79a**.[84] Salicylic iron complex **80b** (Fig. 16) showed significant photocytotoxicity in visible light (400–700 nm) giving IC_{50} values of 8.6 and 3.4 μM in HeLa and MCF-7 cells. It also displayed cytosolic localization with the possibility of mitochondrial DNA being the target.[85] In order to achieve the targeted mitochondrial intrinsic apoptotic pathway, a cationic lipophilic triphenylphosphonium (TPP) moiety was introduced as a pendant to design a new iron(III) catecholate **81** (Fig. 16). Complex **81** displayed mitochondrial localization, ROS generation under red light, and apoptotic cell death.[86]

The higher rate of glucose metabolism is a general characteristic of tumor cells. Conjugation of glucose to the ligand could ensure higher uptake of the iron complex in tumor cells and increase its aqueous solubility. Glucose-conjugated complexes **82** (Fig. 16) were found to show better photocytotoxicity against HeLa cells compared to non-glucose analogues under identical experimental conditions. This is due to the preferential internalization of complexes **82** in tumor cells.[87] Rapidly proliferating malignant tumor cells are in need of excessive consumption of numerous nutrients. With an objective to achieve selective uptake in cancer cells, Basu synthesized new iron(III) complexes **83** (Fig. 16) of the vitamin B6 (VB6) ligand and investigated their cellular uptake and photocytotoxicity.[88] Complexes **83** displayed exceptional photocytotoxicity in the three tested tumor cell lines with IC_{50} values ranging from 3 to 7 μM in visible light (400–700 nm). It was observed that complexes **83** accumulated inside the endoplasmic reticulum of HeLa cells. This could induce an ER stress response by generating ROS after irradiation.[88] Diiodo complex **84** (Fig. 16) induced photocytotoxicity in the presence of visible light with IC_{50} values in the range of 0.11–0.25 μM, which was about 200-fold lower than that in the absence of light.[89] The oxo-bridged binuclear iron(III) complex **85** (Fig. 16) also showed promising photocytotoxicity in HeLa and MCF-7 cells under visible light, while its dark toxicity was negligible.[90]

6.2 Fe(III) complexes with ENN tridentate ligands

Iron(III) complexes **86** (Fig. 17) with Schiff base tridentate ligands derived from phenolato donor(s) displayed efficient chemical nuclease activities in the absence of an oxidising or a reducing agent. Further *in vitro* cytotoxicity studies showed

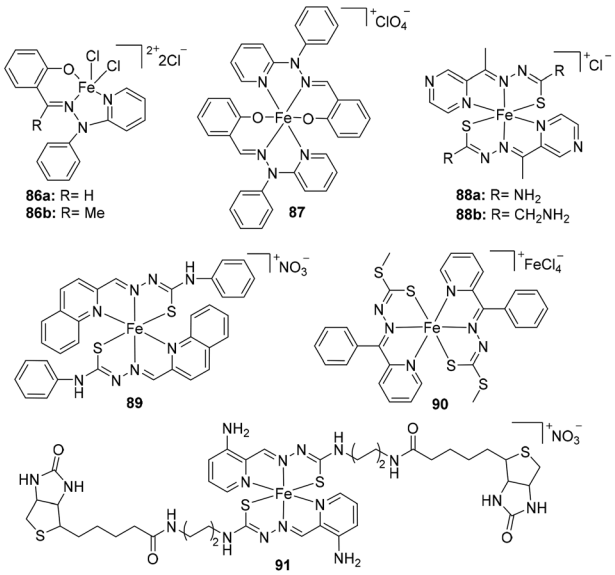

Fig. 17 Fe(III) complexes with ENN tridentate ligands as antitumor agents.

that they were non-toxic to the normal HEK cell line, but exhibited anti-proliferative activity against the MCF-7 cell line with an IC_{50} value of ~0.46 μM for 24 h.[91] While bis-chelated complex **87** (Fig. 17) is not as effective as mono-chelated complexes **86**.[91] In view of the widespread application of thiosemicarbazones in antitumor research, Li *et al.*[92] synthesized octahedrally hexacoordinated iron(III) complexes **88** (Fig. 17) through the coordination of the sulfur atom and two nitrogen atoms in each thiosemicarbazone with iron ions. Complexes **88a**[92b] and **88b**[92a] exhibited cytotoxicity against human esophagus Ec9706 carcinoma cell and hepatoma BEL-7402 cell lines, respectively. The α-N-heterocyclic thiosemicarbazone iron complex **89** (Fig. 17) induced apoptosis through DNA damage and ROS overproduction. It is much more cytotoxic than cisplatin with IC_{50} values of ~0.23 μM for the selected cell lines for 48 h.[93] However, the activity of iron complex **90** (Fig. 16) was only similar to cisplatin toward the A549 lung cancer cell line. The free ligands caused cancer cell death with potency even higher than the corresponding iron(III) complex.[94] To increase tumor specificity and accumulation, Kowol *et al.*[95] prepared biotin-conjugated thiosemicarbazone iron complex **91** (Fig. 17). Disappointingly, complex **91** showed a significant plummet in activity without determined reason compared to non-metallated biotin. The structure–activity relationship of thiosemicarbazone iron complexes still needs further exploration.

7 Pincer Ru(II) complexes

7.1 Mononuclear ruthenium complexes

Ruthenium complexes have been considered as promising metal drugs in cancer treatment since they preferentially loca-

lize in tumor tissues. Many polypyridyl ruthenium complexes have been studied for cytotoxicity,[96] which has aroused great interest from researchers. Complex **92** containing a terpyridine ligand (Fig. 18) exhibited IC_{50} values as low as micromolar to murine L1210 leukemia.[96a] Further research studies revealed that it binds two guanine derivatives in trans configuration to form interchain cross-links in DNA.[96b] Alessio *et al.*[96c] prepared complexes **93** (Fig. 18) with the general formula *mer*-[Ru(terpy)(NN)Cl]Cl, where NN = ethylenediamine (**93a**), 1,2-diaminocyclohexane (**93b**) or 2,2′-bipyridine (**93c**). The MTT assay results indicated that complexes **93a** and **93b** exhibited moderate cytotoxicity against A549, HCT116, and CT26 cell lines, while complex **93c** lost its activity (Table 13).[96d] Complexes **93a** and **93b** interacted with calf thymus DNA strongly, which suggested that DNA may be the target of these types of complexes. Research studies on their interaction with transport proteins, such as serum albumin and transferrin, indicate that they prefer albumin, and complexes **93a** and **93b** have higher affinity for human serum albumin (HAS) than complex **93c**, which proved that they may have multiple targets and mechanisms.[96g]

In order to further investigate whether the modified polypyridyl tridentate ligand will affect the cytotoxicity of the complexes, Ru(II) chlorophenyl terpyridine complexes **94** (Fig. 18) were synthesized and their cytotoxicities against HeLa and A549 cells were evaluated. Interestingly, complex **94c** displayed the highest cytotoxicity among them (Table 14), which was in contrast to the previous complexes (**93**) with chloro terpyridine ligands.[96f] Introducing a chlorophenyl substituent into the terpyridine ligand enhanced the antitumor activity.[96e] This may be related to the lipophilicity of the complexes. Higher lipophilicity promotes cell uptake of drugs, thereby enhancing their anticancer properties.

NHCs are widely used in the design of metal coordination compounds. A pyridine-bridged benzimidazole CNC pincer ligand exhibited remarkable cytotoxicity when coordinated with ruthenium ions (**95**) (Fig. 18). Its IC_{50} values are much lower than that of the corresponding platinum complex **10**, even cisplatin and carboplatin.[21] Upon replacement of the bridged pyridine group with a pyrazine group, complex **96** (Fig. 18) was found to inhibit cell proliferation in a concen-

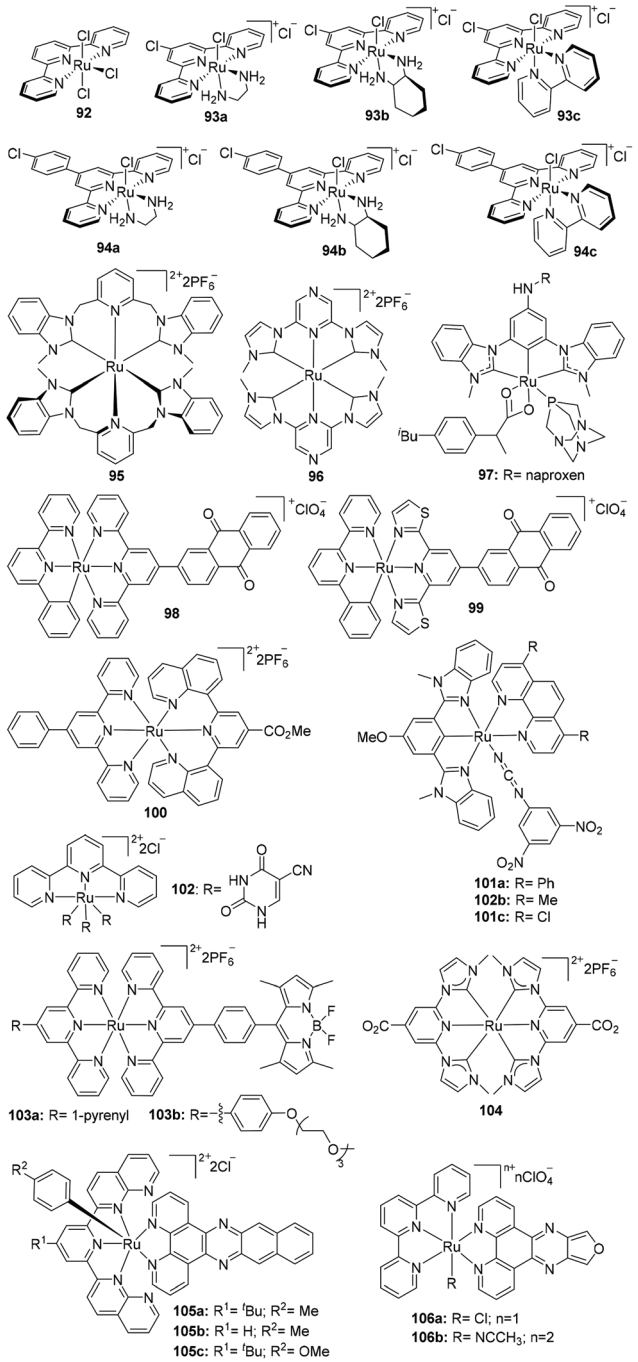

Fig. 18 Mononuclear pincer Ru(II) complexes as antitumor agents.

Table 13 IC_{50} values (μM) of the pincer Ru(II) complexes (**93**) toward three human tumor cell lines[96d]

	IC_{50} value[a] (μM)		
Complex	A549	HCT116	CT26
93a	58.4	66.3	32.8
93b	>100	84.4	72.8
93c	>100	>100	>100

[a] Incubation for 72 h at 37 °C with 5% CO_2.

Table 14 IC_{50} values (μM) of the pincer Ru(II) complexes (**94**) toward three human cell lines[96f]

	IC_{50} value[a] (μM)		
Complex	HeLa	A549	MRC-5
94a	84.81	>100	>100
94b	96.28	>100	>100
94c	12.68	53.80	97.67

[a] Incubation for 72 h at 37 °C with 5% CO_2.

tration-dependent manner. Its activity is better than those of the corresponding benzimidazole analogues.[97] Following the inspiration of the reports about the unique anti-metastatic activity of new ruthenium complexes with 1,3,5-triaza-7-phosphaadamantane (PTA),[98] Tabrizi *et al.* designed and synthesized a new cyclometalated Ru(II)-PTA complex **97** (Fig. 18). It was observed that **97** was selective for MCF-7 and MDA-MB-231 breast cancer cell lines compared to HT-29 colon cancer cell lines, with IC_{50} values (72 h) as low as ~0.91 μM. Moreover, its cytotoxicity against human embryonic kidney HEK293 cells is much lower than that of cisplatin, with an IC_{50} value of >100 μM.[99]

The hypoxic environment in tumors plays a very important role in the development of drug resistance. Doxorubicin, an anthraquinone derivative, is widely used in the treatment of solid tumors. Chao *et al.* integrated anthraquinones with cyclometalation to develop a series of pincer ruthenium complexes. Among them, complexes **98** and **99** (Fig. 18) maintained strong antitumor activity even in a hypoxic environment. Their activity was significantly correlated with lipophilicity and cell uptake. Complex **98** containing a 2,2′:6′,2″-terpyridine ligand is more toxic than complex **99** containing a 2,6-di(thiazol-2-yl) pyridine ligand, because the sulfur atoms in complex **99** are more hydrophilic.[100]

Ruthenium(II) with a d^6 electronic structure has the characteristics of a large Stokes shift, long phosphorescence lifetime, excellent photostability and high $^1O_2$ quantum yield.[101] Therefore, Ruthenium(II) compounds are of great interest in photodynamic therapy. Frei *et al.*[102] demonstrated that NNN tridentate pincer Ru complex **100** (Fig. 18) exhibited high phototoxicity in the low micromolar range against HeLa cells upon 420 nm irradiation, even though its cellular uptake was not so much. Its phototoxic index (PI) is as high as 80. Appropriate modification to increase its cellular uptake may further induce enhanced phototoxicity. Tabrizi has recently reported a series of ruthenium complexes (**101**) of phenylcyanamide derivatives (Fig. 18) that induce the formation of $^1O_2$ and $^{\bullet}OH$ under light activation. Among them, **101a** showed the highest phototoxicity in HeLa cells, with a PI of 94 upon 420 nm irradiation.[103]

In order to improve the potential of pincer ruthenium(II) complexes in PDT applications, researchers have made efforts in some aspects. NNN pincer ruthenium complex **102** (Fig. 18) was observed to release one 5-cyanuracil ligand upon irradiation, which was structurally related to the clinical 5-fluorouracil antitumor agent. The phototoxicity of **102** is almost the same as that of free 5-cyanuracil, which proves that the 5-cyanuracil released is responsible for the toxicity of **102**.[104] Liu *et al.*[105] incorporated the boron dipyrromethene (BODIPY) motif into a 4-phenyl terpyridine in pincer Ru(II) complexes (**103**) (Fig. 18), prolonging lifetimes of their lowest triplet excited states. The PIs of **103a** and **103b** in A549 cells were 4.9 and 35.3, respectively, irradiated with 500 nm light of 0.48 J cm^{-2} for 10 min. Compared with **103a**, **103b** can induce the production of $^1O_2$ more efficiently.[105] An NHC with strong σ-donor ability replaced the terpyridine ligand and coordinated with Ru iron to form CNC pincer ruthenium complex **104** (Fig. 18). It significantly increased the excited state lifetime, which was about 2660-fold longer than that of the terpyridine ruthenium complex. The phototoxicity of **104** under 405 nm irradiation was similar to that of cisplatin with PI > 86 in the human promyelocytic leukaemia HL60 cell line.[106] This result proved that it is feasible to incorporate NHCs into metal complexes for PDT application.

To expand the application of PDT in deep tumor tissues, researchers are committed to expanding the PDT window to the NIR region. Melanoma cells, that absorb and attenuate light effectively, are somewhat resistant to PDT. The design of photosensitizers with high $^1O_2$ quantum yield in the NIR region is critical for the treatment of melanoma. NNN tridentate pincer Ru(II) complexes **105** (Fig. 18) with π-expansion orthogonal to the direction of the M–N bond were found such that the energy of their triplet intraligand (3IL) states was lower than that of the lowest triplet metal–ligand charge transfer (3MLCT) excited states. **105** displayed micromolar phototoxicity toward melanoma cells upon NIR 733 nm irradiation. However, **105** lost photocytotoxicity under hypoxic conditions regardless of light irradiation.[107] The hypoxic environment of tumor tissue limits the efficacy of PDT agents. Yu *et al.*[108] recently reported that two NNN pincer ruthenium complexes (**106**) (Fig. 18) simultaneously cleaved DNA through oxygen-dependent and independent pathways under light irradiation. The presence of various free radical scavengers under anaerobic conditions did not have any effect on the photocleavage of **106**. Oxygen-independent PDT agents **106** may become more promising candidates for the treatment of hypoxic tumors.

7.2 Multinuclear ruthenium complexes

To increase the cytotoxicity of the mononuclear ruthenium complexes, the researchers tried to focus on the multinuclear ruthenium complexes. The IC_{50} values (48 h) of binuclear ruthenium complexes **107a** (Fig. 19) determined to be 4.2–9.9 μM are almost 12-fold that of the L1210 murine leukaemia cell line compared with the corresponding mononuclear complex $[Ru(terpy)(Me_2bpy)Cl]^+$ (IC_{50} = 50 μM).[109] Complexes **107b** (Fig. 19) obtained by modifying terpyridine rings with nitro substituents were found to decrease the cytotoxicity toward MCF-7 and MDA-MB-231 breast cancer cell lines. Complexes **108** (Fig. 19) obtained by replacing two methylene groups on the linking bridge with amino groups also reduced toxicity. When n = 12, the complex was the most active. The complexes with a shorter linking bridge (n = 7 or 10) and a longer linking bridge (n = 14 or 16) show lower activity. This may be due to the best compromise between the lipophilicity of the complex (for cellular uptake) and the cytotoxicity caused by covalent binding to DNA when n = 12.[110]

8 Pincer Ni(II) complexes

Nickel is often chosen as a metal element in the study of metal coordination complexes. With increasing attention towards

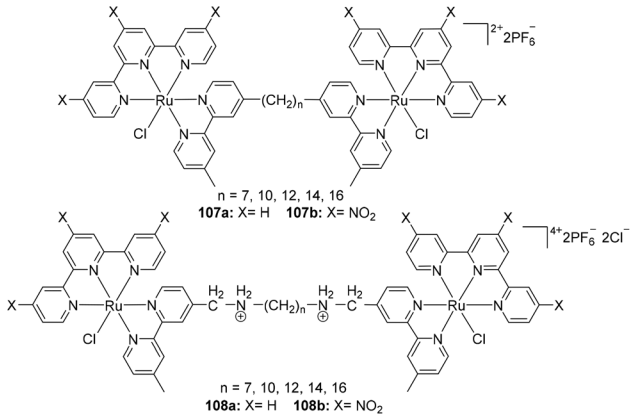

Fig. 19 Multinuclear pincer Ru(II) complexes as antitumor agents.

pincer ligands in metal complexes, pincer nickel complexes as antitumor agents have also attracted interest from researchers. For instance, Milenković *et al.*[111] prepared PNO pincer Ni(II) complexes **109** (Fig. 20) with the condensation derivative of 2-(diphenylphosphino)benzaldehyde and ethyl carbazate. The pseudohalide anion (azide, cyanate and thiocyanate) at the fourth coordination position were altered to study the effects on their antitumor activity. In particular, azido complex **109c** showed selective cytotoxicity to K562 cells with an IC_{50} value similar to that of cisplatin. However, analogues **110** (Fig. 20) were observed to be most active against HeLa cells.[112] Slight structural changes in the pincer ligand may result in significant differences in biological activity due to their lipophilicity and stability. The PNP pincer nickel complex **111** (Fig. 20) based on bis[(2-diphenylphosphino)ethyl] amine exhibited a square-planar geometry. Its cytotoxicity against MCF-7 and HT-29 cancer cells depends on the culture time and concentration. It was found that a low concentration (50 μl) complex **111**·EtOH gave the highest cancer cell death efficiency in less time (24 h) on MCF-7 cancer cells.[113]

In addition to the triphenylphosphine moiety involved in the composition of the pincer ligand, Li *et al.*[114] also prepared ONO pincer nickel complexes **112** (Fig. 20), in which one triphenylphosphine was coordinated directly with the central nickel as an ancillary ligand. Complex **112a** was found to show more effective cytotoxicity against MCF-7 cells (IC_{50} = 9.8 μM for 48 h), and its activity was superior to that of cisplatin.[114]

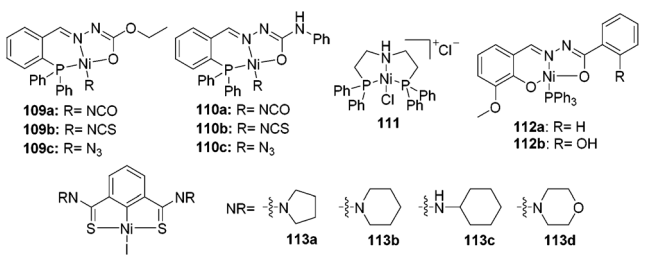

Fig. 20 Pincer Ni(II) complexes as antitumor agents.

Four thioamide based SCS-type pincer ligands featuring various amine fragments and their Ni(II) complexes **113** (Fig. 20) have been evaluated for their potential as antitumor agents.[115] MTT analysis suggested that complex **113a** containing pyrrolidine fragments was most cytotoxic to breast MCF-7 cancer cells. Also, complex **113a** significantly inhibited the proliferation of estrogen-dependent cancer cells in female BALB/c mice,[115a] while the activity of Ni complex **113c** is reduced compared to its free ligand.[115b]

9 Other metal complexes with tridentate ligands

In addition to the metals mentioned above, some other metal complexes containing tridentate ligands also exhibited antitumor activity. For instance, Boff *et al.*[116] synthesized numerous osmium complexes and studied their structure–activity relationships. Among them, complexes **114–116** (Fig. 21) containing an NNN or NCN pincer ligand showed cytotoxicity against human glioblastoma A172 cells comparable to cisplatin. The substitution of electron-donating groups (*e.g.*, dimethylamino of **114b**) on 2-phenylpyridine resulted in relatively increased cytotoxicity. However, modifications on the tridentate pincer NCN or NNN ligands had a negligible effect. Complex **116** with an osmium center coordinated with both NCN and NNN pincer ligands showed the strongest antiproliferative activity.[116] NCN pincer iridium(III) complexes **117** with *meso*-phenylcyanamide BODIPY ligands (Fig. 21) were much less toxic to HeLa cells in the dark (IC_{50} = ~60 μM) than they are under 500 nm irradiation (IC_{50} = ~0.5 μM). They can form $^1O_2$ under photoactivation to contribute to SC-DNA cleavage.[117]

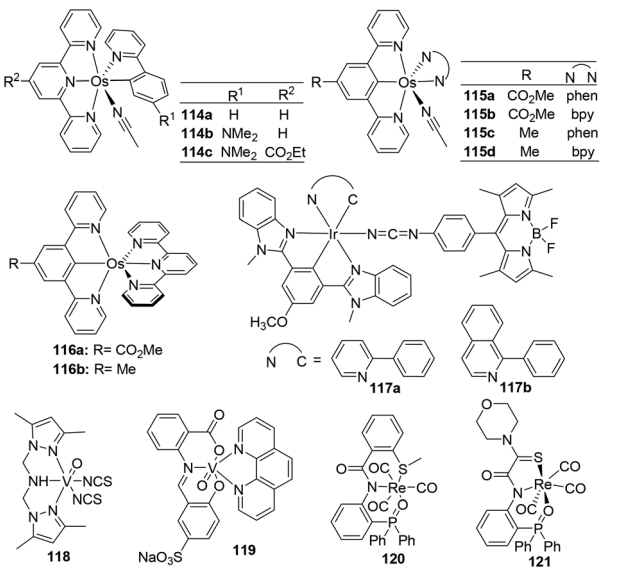

Fig. 21 Other metal complexes with tridentate ligands as antitumor agents.

Vanadium and its complexes are involved in the study of anti-diabetic properties due to their insulin-like effects. In recent years, it has been found that vanadium complexes also have antitumor activity, especially oxovanadium (VO) complexes have gained more attention. Adach *et al.*[118] synthesized NNN pincer VO complex **118** (Fig. 21) *via* a simple one-pot process for the first time. Biological results showed that the cytotoxicity of **118**·toluene were significantly higher than that of vanadium salt ($VOSO_4$). VO complex **119** coordinated with an ONO pincer ligand derived from Schiff base (Fig. 21) even exhibited remarkable antiproliferative potential comparable to the standard anticancer reagent vinblastine.[119]

Rhenium(I) and its complexes have also been reported in anticancer drug development. Aleksanyan demonstrated that non-toxic free monothiooxamide ligands coordinated with Re (I) ions (**120** and **121**) (Fig. 21) exhibited significant toxic effects on human colon HCT116, breast MCF7, and prostate PC3 cancer cell lines. Their activity was higher than clinical cisplatin with IC_{50} values within the low micromolar range.[120] Moreover, no interaction between complex **121** and DNA was observed.[120a] Unfortunately, complexes **120** and **121** did not show selectivity against human embryonic kidney HEK293 cells.[120] Reasonable design to improve the selectivity of metal coordinated complexes is the direction of future efforts.

10 Conclusions

This review summarizes the significant progress in the research studies of the antitumor activity of pincer and related platinum(II), gold(III), palladium(II), copper(II), iron(III), ruthenium(II), nickel(II) and some other metal complexes. The coordination number, redox potential, and unique kinetic and thermodynamic properties of transition metals have attracted extensive attention. Modifications of various functionalized ligands give promising cytotoxicity to metal compounds. Pincer tridentate ligands can effectively improve the stability of metal compounds. Moreover, their easy regulation makes the development of antitumor drugs more possible and convenient. In addition to modifications on the pincer ligands, the introduction of functional auxiliary ligands (such as NHCs) at the coordinated sites of central metals is also a feasible design idea. With the increasing in-depth research studies on the mechanism of transition metal complexes, different metal centers seem to have diverse biological targets. For instance, platinum(II) and palladium(II) mainly target DNA, while gold(III) prefers thiol–enzymes. The unique optical properties of ruthenium also make it widely studied in PDT. These mechanisms of action may become a breakthrough point in overcoming drug resistance in the future. However, the current research studies on the targets and mechanisms of metal coordination complexes are still very shallow. The development of drugs with different pharmacological targets to overcome resistance is the direction of future efforts to design pincer and related metal compounds.

Abbreviations

IC_{50}	Half maximal inhibitory concentration
GI_{50}	50% Growth inhibition
MTT	3-(4,5-Dimethylthiazol-2-yl)-2,5diphenyltetrazolium bromide
CREB	cAMP response element binding protein
TNF-α	Tumor necrosis factor-α
NF-κB	Nuclear factor κB
Topo	Topoisomerase
TrxR	Thioredoxin reductase
CT-DNA	Calf-thymus DNA
BSA	Bovine serum albumin
GSH	Glutathione
ALT	Alanine aminotransferase
AST	Aspartate aminotransferase
VEGF	Vascular endothelial growth factor
ER stress	Endoplasmic reticulum stress
HSA	Human serum albumin
PDT	Photodynamic therapy
PS	Photosensitizer
PI	Phototoxic index
NIR	Near-infrared
ROS	Reactive oxygen species
$^{\bullet}OH$	Hydroxyl radicals
$^1O_2$	Singlet oxygen
VB6	Vitamin B6
3IL	Triplet intraligand
3MLCT	Triplet metal–ligand charge transfer
Me	Methyl
Et	Ethyl
^{n}Bu	*n*-Butyl
^{t}Bu	*tert*-Butyl
^{n}Pr	*n*-Propyl
^{i}Pr	Isopropyl
Cy	Cyclohexyl
Bn	Benzyl
Ph	Phenyl
dien	Diethylenetriamine
NHC	N-Heterocyclic carbene
terpy	2,2′:6′,2″-Terpyridine
bpy	2,2′-Bipyridine
phen	1,10-Phenanthroline
dpq	Dipyrido[3,2-f:2′,3′-h]quinoxaline
dppz	Dipyrido[3,2-a:2′,3′-c]phenazine
dmdppz	11,12-Dimethyldipyrido[3,2-*a*:2′,3′-*c*]phenazine
TPP	Triphenylphosphonium
PTA	1,3,5-Triaza-7-phosphaadamantane
BODIPY	Boron dipyrromethene
HeLa	Human cervical cancer cell line
MCF-7	Human breast cancer cell line
A549	Human lung carcinoma cancer cell line
MDA-MB-231	Human breast adenocarcinoma cell line
HT-29	Colorectal adenocarcinoma cell line
HepG2	Hepatocellular carcinoma cell
PC3	Prostate cancer cell line

HCT116	Human colon carcinoma cell line
CT26	Mouse colon carcinoma cell line
BEL-7402	Human hepatoma cell line
SUNE1	Human nasopharyngeal carcinoma cell line
NCI-H460	Non-small-cell lung carcinoma cell line
CCD-19Lu	Human normal lung fibroblast cell line
AY27	Rat bladder tumor cell line
Caov-3	Human ovarian cancer cell line
T24	Human bladder cancer cell line
A2780	Human ovarian cancer cell line
CNE1	Human nasopharyngeal carcinoma cell line
B16	Mouse melanoma cell line
HL60	Human leukaemia cell line
K562	Human erythroleukemic cell line
U251	Human glioma cell line
TOV21G	Human ovarian cell line
SW620	Human colon carcinoma cell line
NCI-H1688	Small-cell lung carcinoma cell line
HEK293	Normal human embryonic kidney cell line
T47D	Human breast cancer cell line
Vero	Monkey kidney cell line
NIH 3T3	Mouse embryonic fibroblast cell line
ME180	Human cervical epidermoid carcinoma cell line
MOLT-4	Human lymphoblastic leukaemia cell line
HEp-2	Human larynx epidermoid carcinoma cell line
COLO-205	Human colon carcinoma cell line
SKLU-1	Human lung carcinoma cell line
AGS	Human gastric carcinoma cell line
KATOIII	Human gastric carcinoma cell line
HCT-15	Human colon carcinoma cell line
Ec9706	Human esophageal carcinoma cell line
HL60	Human promyelocytic leukaemia cell line
L1210	Murine leukaemia cell line
A172	Human glioblastoma cell line

Conflicts of interest

There are no conflicts to declare.

Acknowledgements

This work was supported by the open fund for innovation platform of Hunan Provincial Department of Education (Grant No. 19K079), the Natural Science Foundation of Hunan Province (Grant No. 2018JJ3426), the young and middle-aged innovative personnel training project of the Hunan Province Cooperative Innovation Center for Molecular Target New Drug Study (Grant No. 0223-0002-0002000-52) and the China Scholarship Council (Grant No. CSC201908430070).

Notes and references

1 F. Bray, J. Ferlay, I. Soerjomataram, R. L. Siegel, L. A. Torre and A. Jemal, *CA Cancer J. Clin.*, 2018, **68**, 394–424.
2 B. Rosenberg, L. Vancamp, J. E. Trosko and V. H. Mansour, *Nature*, 1969, **222**, 385–386.
3 A. M. Florea and D. Busselberg, *Cancers*, 2011, **3**, 1351–1371.
4 (*a*) L. Kelland, *Nat. Rev. Cancer*, 2007, **7**, 573–584; (*b*) N. J. Wheate, S. Walker, G. E. Craig and R. Oun, *Dalton Trans.*, 2010, **39**, 8113–8127.
5 J. Sophie, E. K. Fritz and C. Angela, *Curr. Med. Chem.*, 2018, **25**, 437–461.
6 (*a*) M. E. Van Der Boom and D. Milstein, *Chem. Rev.*, 2003, **103**, 1759–1792; (*b*) J. T. Singleton, *Tetrahedron*, 2003, **59**, 1837–1857; (*c*) N. Selander and K. J. Szabó, *Chem. Rev.*, 2011, **111**, 2048–2076; (*d*) Y. Xu, Z. Yang, B. Ding, D. Liu, Y. Liu, M. Sugiya, T. Imamoto and W. Zhang, *Tetrahedron*, 2015, **71**, 6832–6839; (*e*) Z. Yang, X. Wei, D. Liu, Y. Liu, M. Sugiya, T. Imamoto and W. Zhang, *J. Organomet. Chem.*, 2015, **791**, 41–45; (*f*) Z. Yang, C. Xia, D. Liu, Y. Liu, M. Sugiya, T. Imamoto and W. Zhang, *Org. Biomol. Chem.*, 2015, **13**, 2694–2702; (*g*) Y. Xiang, Q. Ge, S. Wu, X. Zheng and Z. Yang, *RSC Adv.*, 2020, **10**, 9563–9578; (*h*) Z. Yang, D. Liu, Y. Liu, M. Sugiya, T. Imamoto and W. Zhang, *Organometallics*, 2015, **34**, 1228–1237; (*i*) M. Asay and D. Moralesmorales, *Dalton Trans.*, 2015, **44**, 17432–17447; (*j*) F. E. Hahn, M. C. Jahnke and T. Pape, *Organometallics*, 2007, **26**, 150–154; (*k*) D. Benitogaragorri and K. Kirchner, *Acc. Chem. Res.*, 2008, **41**, 201–213.
7 (*a*) A. R. Kapdi and I. J. S. Fairlamb, *Chem. Soc. Rev.*, 2014, **43**, 4751–4777; (*b*) N. Cutillas, G. S. Yellol, C. De Haro, C. Vicente, V. Rodríguez and J. Ruiz, *Coord. Chem. Rev.*, 2013, **257**, 2784–2797; (*c*) S. Medici, M. Peana, V. M. Nurchi, J. I. Lachowicz, G. Crisponi and M. A. Zoroddu, *Coord. Chem. Rev.*, 2015, **284**, 329–350; (*d*) T. Lazarević, A. Rilak and Ž. D. Bugarčić, *Eur. J. Med. Chem.*, 2017, **142**, 8–31.
8 D. a. K. Vezzu, Q. Lu, Y. Chen and S. Huo, *J. Inorg. Biochem.*, 2014, **134**, 49–56.
9 W. Liu and R. Gust, *Chem. Soc. Rev.*, 2013, **42**, 755–773.
10 R. W. Sun, A. L. Chow, X. Li, J. J. Yan, S. S. Chui and C. Che, *Chem. Sci.*, 2011, **2**, 728–736.
11 J. Quirante, D. Ruiz, A. Gonzalez, C. López, M. Cascante, R. Cortés, R. Messeguer, C. Calvis, L. Baldomà, A. Pascual, Y. Guérardel, B. Pradines, M. Font-Bardía, T. Calvet and C. Biot, *J. Inorg. Biochem.*, 2011, **105**, 1720–1728.
12 W. Hu, X.-S. Huang, J.-F. Wu, L. Yang, Y.-T. Zheng, Y.-M. Shen, Z.-Y. Li and X. Li, *J. Med. Chem.*, 2018, **61**, 8947–8980.
13 P. Wang, C. Leung, D. Ma, W. Lu and C. Che, *Chem. – Asian J.*, 2010, **5**, 2271–2280.
14 L. Mélanie, J. Samy, D. Sabine and D. C. Marie-Hélène, *Molecules*, 2018, **23**, 1479.
15 P. Wang, C. Leung, D. Ma, R. W. Sun, S. Yan, Q. Chen and C. Che, *Angew. Chem., Int. Ed.*, 2011, **50**, 2554–2558.
16 J. Liu, R. W. Sun, C. Leung, C. Lok and C. Che, *Chem. Commun.*, 2012, **48**, 230–232.
17 T. Zou, J. Liu, C. T. Lum, C. Ma, R. C. Chan, C. Lok, W. M. Kwok and C. Che, *Angew. Chem., Int. Ed.*, 2014, **53**, 10119–10123.

18 P. Tran, S.-E. Lee, D.-H. Kim, Y.-C. Pyo and J.-S. Park, *J. Pharm. Investig.*, 2020, **50**, 261–270.
19 C. Lok, T. Zou, J. Zhang, I. W. Lin and C. Che, *Adv. Mater.*, 2014, **26**, 5550–5557.
20 J. L. Tsai, T. Zou, J. Liu, T. Chen, A. O. Chan, C. Yang, C. Lok and C. Che, *Chem. Sci.*, 2015, **6**, 3823–3830.
21 J. Dinda, S. D. Adhikary, G. Roymahapatra, K. Nakka and M. K. Santra, *Inorg. Chim. Acta*, 2014, **413**, 23–31.
22 S. Garbe, M. Krause, A. Klimpel, I. Neundorf, P. Lippmann, I. Ott, D. Brünink, C. A. Strassert, N. L. Doltsinis and A. Klein, *Organometallics*, 2020, **39**, 746–756.
23 Y. Zhu, M. Zhang, L. Luo, M. R. Gill, C. De Pace, G. Battaglia, Q. Zhang, H. Zhou, J. Wu, Y. Tian and X. Tian, *Theranostics*, 2019, **9**, 2158–2166.
24 R. Doherty, I. V. Sazanovich, L. K. Mckenzie, A. S. Stasheuski, R. Coyle, E. Baggaley, S. Bottomley, J. A. Weinstein and H. E. Bryant, *Sci. Rep.*, 2016, **6**, 22668–22668.
25 K. Li, T. Zou, Y. Chen, X. Guan and C. Che, *Chem. – Eur. J.*, 2015, **21**, 7441–7453.
26 T. Chatzisideri, S. Thysiadis, S. Katsamakas, P. Dalezis, I. Sigala, T. Lazarides, E. Nikolakaki, D. Trafalis, O. A. Gederaas, M. Lindgren and V. Sarli, *Eur. J. Med. Chem.*, 2017, **141**, 221–231.
27 M. A. Ali, A. H. Mirza, R. J. Butcher and K. A. Crouse, *Transition Met. Chem.*, 2006, **31**, 79–87.
28 D. Kovala-Demertzi, A. Papageorgiou, L. Papathanasis, A. Alexandratos, P. Dalezis, J. R. Miller and M. A. Demertzis, *Eur. J. Med. Chem.*, 2009, **44**, 1296–1302.
29 A. Castineiras, N. Fernandez-Hermida, I. Garcia-Santos and L. Gomez-Rodriguez, *Dalton Trans.*, 2012, **41**, 13486–13495.
30 G. L. Parrilha, K. S. O. Ferraz, J. A. Lessa, K. N. De Oliveira, B. L. Rodrigues, J. P. Ramos, E. M. Souza-Fagundes, I. Ott and H. Beraldo, *Eur. J. Med. Chem.*, 2014, **84**, 537–544.
31 F.-U. Rahman, A. Ali, H.-Q. Duong, I. U. Khan, M. Z. Bhatti, Z.-T. Li, H. Wang and D.-W. Zhang, *Eur. J. Med. Chem.*, 2019, **164**, 546–561.
32 T. M. Simon, D. H. Kunishima, G. J. Vibert and A. Lorber, *Cancer*, 1979, **44**, 1965–1975.
33 S. Nobili, E. Mini, I. Landini, C. Gabbiani, A. Casini and L. Messori, *Med. Res. Rev.*, 2009, **30**, 550–580.
34 (*a*) L. Messori, F. Abbate, G. Marcon, P. Orioli, M. Fontani, E. Mini, T. Mazzei, S. Carotti, T. Oconnell and P. Zanello, *J. Med. Chem.*, 2000, **43**, 3541–3548; (*b*) L. Messori, P. Orioli, C. Tempi and G. Marcon, *Biochem. Biophys. Res. Commun.*, 2001, **281**, 352–360; (*c*) G. Marcon, L. Messori, P. Orioli, M. A. Cinellu and G. Minghetti, *FEBS J.*, 2003, **270**, 4655–4661.
35 T. Zou, C. T. Lum, S. S. Chui and C. Che, *Angew. Chem., Int. Ed.*, 2013, **52**, 2930–2933.
36 S. Radisavljevic, I. Bratsos, A. Scheurer, J. Korzekwa, R. Masnikosa, A. Tot, N. Gligorijevic, S. Radulovic and A. Simovic, *Dalton Trans.*, 2018, **47**, 13696–13712.
37 G. Marcon, S. Carotti, M. Coronnello, L. Messori, E. Mini, P. Orioli, T. Mazzei, M. A. Cinellu and G. Minghetti, *J. Med. Chem.*, 2002, **45**, 1672–1677.
38 M. Coronnello, E. Mini, B. Caciagli, M. A. Cinellu, A. Bindoli, C. Gabbiani and L. Messori, *J. Med. Chem.*, 2005, **48**, 6761–6765.
39 C. Gabbiani, L. Massai, F. Scaletti, E. Michelucci, L. Maiore, M. A. Cinellu and L. Messori, *J. Biol. Inorg. Chem.*, 2012, **17**, 1293–1302.
40 C. Gabbiani, F. Scaletti, L. Massai, E. Michelucci, M. A. Cinellu and L. Messori, *Chem. Commun.*, 2012, **48**, 11623–11625.
41 T. Gamberi, L. Massai, F. Magherini, I. Landini, T. Fiaschi, F. Scaletti, C. Gabbiani, L. Bianchi, L. Bini, S. Nobili, G. Perrone, E. Mini, L. Messori and A. Modesti, *J. Proteomics*, 2014, **103**, 103–120.
42 L. Messori, G. Marcon, M. A. Cinellu, M. Coronnello, E. Mini, C. Gabbiani and P. Orioli, *Bioorg. Med. Chem.*, 2004, **12**, 6039–6043.
43 P. Gratteri, L. Massai, E. Michelucci, R. Rigo, L. Messori, M. A. Cinellu, C. Musetti, C. Sissi and C. Bazzicalupi, *Dalton Trans.*, 2015, **44**, 3633–3639.
44 C. K.-L. Li, R. W.-Y. Sun, S. C.-F. Kui, N. Zhu and C.-M. Che, *Chem. – Eur. J.*, 2006, **12**, 5253–5266.
45 J. J. Yan, A. L. Chow, C. Leung, R. W. Sun, D. Ma and C. Che, *Chem. Commun.*, 2010, **46**, 3893–3895.
46 S. K. Fung, T. Zou, B. Cao, P.-Y. Lee, Y. M. E. Fung, D. Hu, C.-N. Lok and C.-M. Che, *Angew. Chem., Int. Ed.*, 2017, **56**, 3892–3896.
47 J. Zhang, W. Lu, R. W. Sun and C. Che, *Angew. Chem., Int. Ed.*, 2012, **51**, 4882–4886.
48 J. L. Tsai, A. O. Chan and C. Che, *Chem. Commun.*, 2015, **51**, 8547–8550.
49 B. Bertrand, J. Fernandezcestau, J. Angulo, M. M. D. Cominetti, Z. a. E. Waller, M. Searcey, M. A. Oconnell and M. Bochmann, *Inorg. Chem.*, 2017, **56**, 5728–5740.
50 E. Guney, V. T. Yilmaz, F. Ari, O. Buyukgungor and E. Ulukaya, *Polyhedron*, 2011, **30**, 114–122.
51 F. Ari, E. Ulukaya, M. Sarimahmut and V. T. Yilmaz, *Bioorg. Med. Chem.*, 2013, **21**, 3016–3021.
52 (*a*) E. Ulukaya, F. Ari, K. Dimas, E. I. Ikitimur, E. Guney and V. T. Yilmaz, *Eur. J. Med. Chem.*, 2011, **46**, 4957–4963; (*b*) E. Ulukaya, F. Ari, K. Dimas, M. Sarimahmut, E. Guney, N. Sakellaridis and V. T. Yilmaz, *J. Cancer Res. Clin. Oncol.*, 2011, **137**, 1425–1434; (*c*) M. D. Coskun, F. Ari, A. Y. Oral, M. Sarimahmut, H. M. Kutlu, V. T. Yilmaz and E. Ulukaya, *Bioorg. Med. Chem.*, 2013, **21**, 4698–4705; (*d*) F. Ari, B. Cevatemre, E. I. Armutak, N. Aztopal, V. T. Yilmaz and E. Ulukaya, *Bioorg. Med. Chem.*, 2014, **22**, 4948–4954; (*e*) O. Kacar, Z. Adiguzel, V. T. Yilmaz, Y. Cetin, B. Cevatemre, N. Arda, A. T. Baykal, E. Ulukaya and C. Acilan, *Anticancer Drugs*, 2014, **25**, 17–29; (*f*) Y. Cetin, Z. Adiguzel, H. U. Polat, T. Akkoc, A. Tas, B. Cevatemre, G. Celik, B. Carikci, V. T. Yilmaz and E. Ulukaya, *Anticancer Drugs*, 2017, **28**, 898–910;

(*g*) E. I. Ikitimurarmutak, E. Gurelgurevin, H. T. Kiyan, S. Aydinlik, V. T. Yilmaz, K. Dimas and E. Ulukaya, *Microvasc. Res.*, 2017, **109**, 26–33; (*h*) O. Kacar, B. Cevatemre, I. Hatipoglu, N. Arda, E. Ulukaya, V. T. Yilmaz and C. Acilan, *Bioorg. Med. Chem.*, 2017, **25**, 1770–1777.

53 F. Darabi, H. Hadadzadeh, J. Simpson and A. Shahpiri, *New J. Chem.*, 2016, **40**, 9081–9097.

54 J. D. Higgins, L. Neely and S. P. Fricker, *J. Inorg. Biochem.*, 1993, **49**, 149–156.

55 J. Vázquez, S. Bernès, P. Sharma, J. Pérez, G. Hernández, A. Tovar, U. Peña and R. Gutiérrez, *Polyhedron*, 2011, **30**, 2514–2522.

56 S. Cruz, S. Bernès, P. Sharma, R. Vazquez, G. Hernández, R. Portillo and R. Gutiérrez, *Appl. Organomet. Chem.*, 2010, **24**, 8–11.

57 N. Lease, V. Vasilevski, M. Carreira, A. De Almeida, M. Sanaú, P. Hirva, A. Casini and M. Contel, *J. Med. Chem.*, 2013, **56**, 5806–5818.

58 M. Frik, J. Jiménez, V. Vasilevski, M. Carreira, A. De Almeida, E. Gascón, F. Benoit, M. Sanaú, A. Casini and M. Contel, *Inorg. Chem. Front.*, 2014, **1**, 231–241.

59 J.-Y. Lee, J.-Y. Lee, Y.-Y. Chang, C.-H. Hu, N. M. Wang and H. M. Lee, *Organometallics*, 2015, **34**, 4359–4368.

60 T. T. Fong, C. Lok, C. Y. Chung, Y. E. Fung, P. Chow, P. Wan and C. Che, *Angew. Chem., Int. Ed.*, 2016, **55**, 11935–11939.

61 L. Yan, X. Wang, Y. Wang, Y. Zhang, Y. Li and Z. Guo, *J. Inorg. Biochem.*, 2012, **106**, 46–51.

62 D. Kovala-Demertzi, A. Galani, J. R. Miller, C. S. Frampton and M. A. Demertzis, *Polyhedron*, 2013, **52**, 1096–1102.

63 S. G. Churusova, D. V. Aleksanyan, E. Y. Rybalkina, O. Y. Susova, V. V. Brunova, R. R. Aysin, Y. V. Nelyubina, A. S. Peregudov, E. I. Gutsul and Z. S. Klemenkova, *Inorg. Chem.*, 2017, **56**, 9834–9850.

64 S. G. Churusova, D. V. Aleksanyan, A. A. Vasil'ev, E. Y. Rybalkina, O. Y. Susova, Z. S. Klemenkova, R. R. Aysin, Y. V. Nelyubina and V. A. Kozlov, *Appl. Organomet. Chem.*, 2018, **32**, e4360.

65 M. Al-Noaimi, F. F. Awwadi, W. H. Talib, S. Atia and H. H. Hammud, *J. Mol. Struct.*, 2019, **1197**, 282–291.

66 P. Kalaivani, R. Prabhakaran, F. Dallemer, P. Poornima, E. Vaishnavi, E. Ramachandran, V. V. Padma, R. Renganathan and K. Natarajan, *Metallomics*, 2012, **4**, 101–113.

67 E. Ramachandran, D. S. Raja, N. P. Rath and K. Natarajan, *Inorg. Chem.*, 2013, **52**, 1504–1514.

68 E. Ramachandran, P. Kalaivani, R. Prabhakaran, N. P. Rath, S. Brinda, P. Poornima, V. V. Padma and K. Natarajan, *Metallomics*, 2012, **4**, 218–227.

69 M. Muralisankar, S. M. Basheer, J. Haribabu, N. S. P. Bhuvanesh, R. Karvembu and A. Sreekanth, *Inorg. Chim. Acta*, 2017, **466**, 61–70.

70 F.-U. Rahman, A. Ali, M. Z. Bhatti, Z.-T. Li, H. Wang and D.-W. Zhang, *Chem. Data Collect.*, 2019, **19**, 100181.

71 P. U. Maheswari, S. Roy, H. Den Dulk, S. Barends, G. P. Van Wezel, B. Kozlevcar, P. Gamez and J. Reedijk, *J. Am. Chem. Soc.*, 2006, **128**, 710–711.

72 (*a*) X. Qiao, Z. Ma, C. Xie, F. Xue, Y. Zhang, J. Xu, Z. Qiang, J. Lou, G. Chen and S. Yan, *J. Inorg. Biochem.*, 2011, **105**, 728–737; (*b*) Z. Ma, X. Qiao, C. Xie, J. Shao, J. Xu, Z. Qiang and J. Lou, *J. Inorg. Biochem.*, 2012, **117**, 1–9.

73 K. Ghosh, P. Kumar, V. Mohan, U. P. Singh, S. Kasiri and S. S. Mandal, *Inorg. Chem.*, 2012, **51**, 3343–3345.

74 M. Alagesan, N. Bhuvanesh and N. Dharmaraj, *Dalton Trans.*, 2013, **42**, 7210–7223.

75 P. Jaividhya, R. Dhivya, M. A. Akbarsha and M. Palaniandavar, *J. Inorg. Biochem.*, 2012, **114**, 94–105.

76 J. Liang, Y. Wang, K. Du, G. Li, R. Guan, L. Ji and H. Chao, *J. Inorg. Biochem.*, 2014, **141**, 17–27.

77 K. Czerwinska, B. Machura, S. Kula, S. Krompiec, K. Erfurt, C. Romarodrigues, A. R. Fernandes, L. S. Shulpina, N. S. Ikonnikov and G. B. Shulpin, *Dalton Trans.*, 2017, **46**, 9591–9604.

78 K. Suntharalingam, D. J. Hunt, A. A. Duarte, A. J. P. White, D. J. Mann and R. Vilar, *Chem. – Eur. J.*, 2012, **18**, 15133–15141.

79 D. S. Raja, G. Paramaguru, N. S. P. Bhuvanesh, J. H. Reibenspies, R. Renganathan and K. Natarajan, *Dalton Trans.*, 2011, **40**, 4548–4559.

80 D. S. Raja, N. S. P. Bhuvanesh and K. Natarajan, *Eur. J. Med. Chem.*, 2011, **46**, 4584–4594.

81 A. H. Pathan, A. K. Ramesh, R. P. Bakale, G. N. Naik, H. G. R. Kumar, C. S. Frampton, G. M. A. Rao and K. B. Gudasi, *Inorg. Chim. Acta*, 2015, **430**, 216–224.

82 A. S. Estrada-Montaño, A. D. Ryabov, A. Gries, C. Gaiddon and R. Le Lagadec, *Eur. J. Inorg. Chem.*, 2017, **2017**, 1673–1678.

83 (*a*) U. Basu, I. Khan, A. Hussain, P. Kondaiah and A. R. Chakravarty, *Angew. Chem., Int. Ed.*, 2012, **51**, 2658–2661; (*b*) U. Basu, I. Pant, I. Khan, A. Hussain, P. Kondaiah and A. R. Chakravarty, *Chem. – Asian J.*, 2014, **9**, 2494–2504.

84 A. Garai, U. Basu, I. Khan, I. Pant, A. Hussain, P. Kondaiah and A. R. Chakravarty, *Polyhedron*, 2014, **73**, 124–132.

85 A. Garai, I. Pant, P. Kondaiah and A. R. Chakravarty, *Polyhedron*, 2015, **102**, 668–676.

86 U. Basu, I. Pant, P. Kondaiah and A. R. Chakravarty, *Eur. J. Inorg. Chem.*, 2016, **2016**, 1002–1012.

87 U. Basu, I. Khan, A. Hussain, B. Gole, P. Kondaiah and A. R. Chakravarty, *Inorg. Chem.*, 2014, **53**, 2152–2162.

88 U. Basu, I. Pant, A. Hussain, P. Kondaiah and A. R. Chakravarty, *Inorg. Chem.*, 2015, **54**, 3748–3758.

89 S. Sahoo, S. Podder, A. Garai, S. Majumdar, N. Mukherjee, U. Basu, D. Nandi and A. R. Chakravarty, *Eur. J. Inorg. Chem.*, 2018, **2018**, 1522–1532.

90 T. Sarkar, R. J. Butcher, S. Banerjee, S. Mukherjee and A. Hussain, *Inorg. Chim. Acta*, 2016, **439**, 8–17.

91 N. Tyagi, A. Chakraborty, U. P. Singh, P. Roy and K. Ghosh, *Org. Biomol. Chem.*, 2015, **13**, 11445–11458.

92 (*a*) L. P. Zheng, C. L. Chen, J. Zhou, M. X. Li and Y. J. Wu, *Z. Naturforsch., B: J. Chem. Sci.*, 2008, **63**, 1257–1261; (*b*) M.-X. Li, J. Zhou, H. Zhao, C.-L. Chen and J.-P. Wang, *J. Coord. Chem.*, 2009, **62**, 1423–1429.
93 Y. Gou, J. Wang, S. Chen, Z. Zhang, Y. Zhang, W. Zhang and F. Yang, *Eur. J. Med. Chem.*, 2016, **123**, 354–364.
94 W. P. Sohtun, T. Khamrang, A. Kannan, G. Balakrishnan, D. Saravanan, M. A. Akhbarsha, M. Velusamy and M. Palaniandavar, *Appl. Organomet. Chem.*, 2020, **34**, e5593.
95 S. Kallus, L. Uhlik, S. Van Schoonhoven, K. Pelivan, W. Berger, A. Enyedy, T. Hofmann, P. Heffeter, C. R. Kowol and B. K. Keppler, *J. Inorg. Biochem.*, 2019, **190**, 85–97.
96 (*a*) O. Novakova, J. Kasparkova, O. Vrana, P. M. Vanvliet, J. Reedijk and V. Brabec, *Biochemistry*, 1995, **34**, 12369–12378; (*b*) P. M. Van Vliet, S. M. S. Toekimin, J. G. Haasnoot, J. Reedijk, O. Novakova, O. Vrana and V. Brabec, *Inorg. Chim. Acta*, 1995, **231**, 57–64; (*c*) A. Rilak, I. Bratsos, E. Zangrando, J. Kljun, I. Turel, Ž. D. Bugarcic and E. Alessio, *Inorg. Chem.*, 2014, **53**, 6113–6126; (*d*) D. Lazic, A. Arsenijevic, R. Puchta, Ž. D. Bugarcic and A. Rilak, *Dalton Trans.*, 2016, **45**, 4633–4646; (*e*) M. M. Milutinovic, S. K. C. Elmroth, G. Davidovic, A. Rilak, O. R. Klisuric, I. Bratsos and Ž. D. Bugarcic, *Dalton Trans.*, 2017, **46**, 2360–2369; (*f*) M. M. Milutinovic, A. Rilak, I. Bratsos, O. R. Klisuric, M. Vranes, N. Gligorijevic, S. Radulovic and Ž. D. Bugarcic, *J. Inorg. Biochem.*, 2017, **169**, 1–12; (*g*) M. Nišavić, M. Stoiljković, I. Crnolatac, M. Milošević, A. Rilak and R. Masnikosa, *Arabian J. Chem.*, 2018, **11**, 291–304.
97 G. Roymahapatra, J. Dinda, A. Mishra, A. Mahapatra, W.-S. Hwang and S. M. Mandal, *J. Cancer Res. Ther.*, 2015, **11**, 105–113.
98 (*a*) V. Ferretti, M. Fogagnolo, A. Marchi, L. Marvelli, F. Sforza and P. Bergamini, *Inorg. Chem.*, 2014, **53**, 4881–4890; (*b*) R. H. Berndsen, A. Weiss, U. K. Abdul, T. J. Wong, P. Meraldi, A. W. Griffioen, P. J. Dyson and P. Nowak-Sliwinska, *Sci. Rep.*, 2017, **7**, 43005.
99 L. Tabrizi, L. O. Olasunkanmi and O. A. Fadare, *Dalton Trans.*, 2019, **48**, 728–740.
100 L. Zeng, Y. Chen, H. Huang, J. Wang, D. Zhao, L. Ji and H. Chao, *Chem. – Eur. J.*, 2015, **21**, 15308–15319.
101 C. Mari, V. Pierroz, R. Rubbiani, M. Patra, J. Hess, B. Spingler, L. Oehninger, J. Schur, I. Ott, L. Salassa, S. Ferrari and G. Gasser, *Chem. – Eur. J.*, 2014, **20**, 14421–14436.
102 A. Frei, R. Rubbiani, S. Tubafard, O. Blacque, P. Anstaett, A. Felgentrager, T. Maisch, L. Spiccia and G. Gasser, *J. Med. Chem.*, 2014, **57**, 7280–7292.
103 L. Tabrizi and H. Chiniforoshan, *Dalton Trans.*, 2016, **45**, 18333–18345.
104 M. A. Sgambellone, A. David, R. N. Garner, K. R. Dunbar and C. Turro, *J. Am. Chem. Soc.*, 2013, **135**, 11274–11282.
105 B. Liu, Y. Gao, M. A. Jabed, S. Kilina, G. Liu and W. Sun, *ACS Appl. Bio Mater.*, 2020, **3**, 6025–6038.
106 R. T. Ryan, K. C. Stevens, R. Calabro, S. Parkin, J. Mahmoud, D. Y. Kim, D. K. Heidary, E. C. Glazer and J. P. Selegue, *Inorg. Chem.*, 2020, **59**, 8882–8892.
107 L. M. Lifshits, J. A. Roque III, P. Konda, S. Monro, H. D. Cole, D. Von Dohlen, S. Kim, G. Deep, R. P. Thummel, C. G. Cameron, S. Gujar and S. A. Mcfarland, *Chem. Sci.*, 2020, **11**, 11740–11762.
108 H.-J. Yu, S.-M. Huang, H. Chao and L.-N. Ji, *J. Inorg. Biochem.*, 2015, **149**, 80–87.
109 Y. Mulyana, G. Collins and R. R. Keene, *J. Incl. Phenom. Macrocycl.*, 2011, **71**, 371–379.
110 A. K. Gorle, A. J. Ammit, L. Wallace, F. R. Keene and J. G. Collins, *New J. Chem.*, 2014, **38**, 4049–4059.
111 M. Milenković, A. Bacchi, G. Cantoni, J. Vilipić, D. Sladić, M. Vujčić, N. Gligorijević, K. Jovanović, S. Radulović and K. Anđelković, *Eur. J. Med. Chem.*, 2013, **68**, 111–120.
112 M. Milenković, A. Pevec, I. Turel, M. Vujčić, M. Milenković, K. Jovanović, N. Gligorijević, S. Radulović, M. Swart, M. Gruden-Pavlović, K. Adaila, B. Čobeljić and K. Anđelković, *Eur. J. Med. Chem.*, 2014, **87**, 284–297.
113 G. Mohammadnezhad, S. Abad, H. Farrokhpour, H. Goerls and W. Plass, *Appl. Organomet. Chem.*, 2021, **35**, e6092.
114 Y. Li, Y. Li, N. Wang, D. Lin, X. Liu, Y. Yang and Q. Gao, *J. Biomol. Struct. Dyn.*, 2020, **38**, 4977–4996.
115 (*a*) M. Hosseini-Kharat, D. Zargarian, A. M. Alizadeh, K. Karami, M. Saeidifar, S. Khalighfard, L. Dubrulle, M. Zakariazadeh, J.-P. Cloutier and Z. Sohrabijam, *Dalton Trans.*, 2018, **47**, 16944–16957; (*b*) M. Hosseini-Kharat, R. Rahimi, D. Zargarian, Z. M. Lighvan, A. A. Momtazi-Borojeni, T. Sharifi, E. Abdollahi, H. Tavakol and T. Mohammadi, *J. Biomol. Struct. Dyn.*, 2019, **37**, 3788–3802.
116 B. Boff, C. Gaiddon and M. Pfeffer, *Inorg. Chem.*, 2013, **52**, 2705–2715.
117 L. Tabrizi and H. Chiniforoshan, *RSC Adv.*, 2017, **7**, 34160–34169.
118 A. Adach, M. Daszkiewicz, M. Tyszka-Czochara and B. Barszcz, *RSC Adv.*, 2015, **5**, 85470–85479.
119 M. S. S. Adam, O. M. El-Hady and F. Ullah, *RSC Adv.*, 2019, **9**, 34311–34329.
120 (*a*) D. V. Aleksanyan, S. G. Churusova, V. V. Brunova, E. Y. Rybalkina, O. Y. Susova, A. S. Peregudov, Z. S. Klemenkova, G. L. Denisov and V. A. Kozlov, *J. Organomet. Chem.*, 2020, **926**, 121498; (*b*) D. V. Aleksanyan, S. G. Churusova, E. Y. Rybalkina, O. I. Artyushin, A. S. Peregudov, Y. V. Nelyubina, Z. S. Klemenkova, O. V. Bykhovskaya and V. A. Kozlov, *J. Organomet. Chem.*, 2019, **892**, 66–74.